R($D^{(*)}$) measurement with hadronic tag

Lin Wang[1], Taichiro Koga[2], R(D*) hadronic tag team
[1]Shandong University
[2]KEK

Jan. 15, 2026 @Belle (II)-China analysis forum

Introduction

- SM expects lepton coupling to EW gauge bosons to be flavor-universal, but tension exists

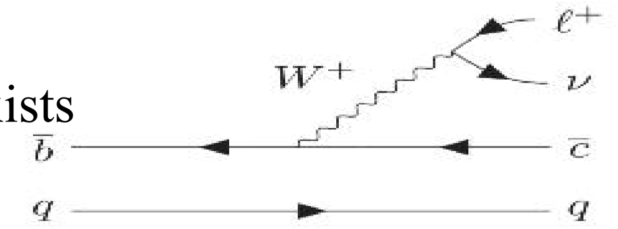

- Tests of LFU are important to search for new physics

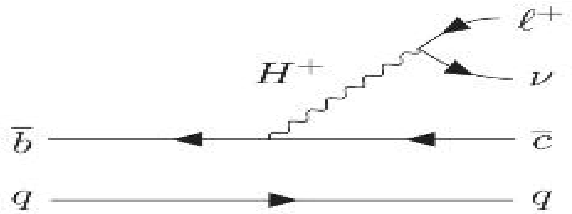

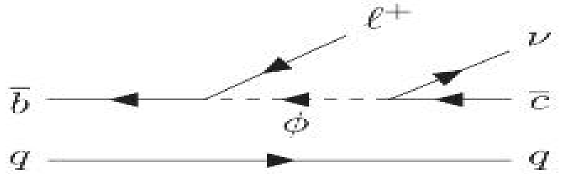

- In the semileptonic decay process of B mesons, $R(D^{(*)})$ is defined as the branching ratio ,

$$R_{D^{(*)}} = \frac{Br(B->D^{(*)}\tau\bar{\nu}_\tau)}{Br(B->D^{(*)}\ell\bar{\nu}_\ell)},$$

where the $\ell = e \; or \; \mu$

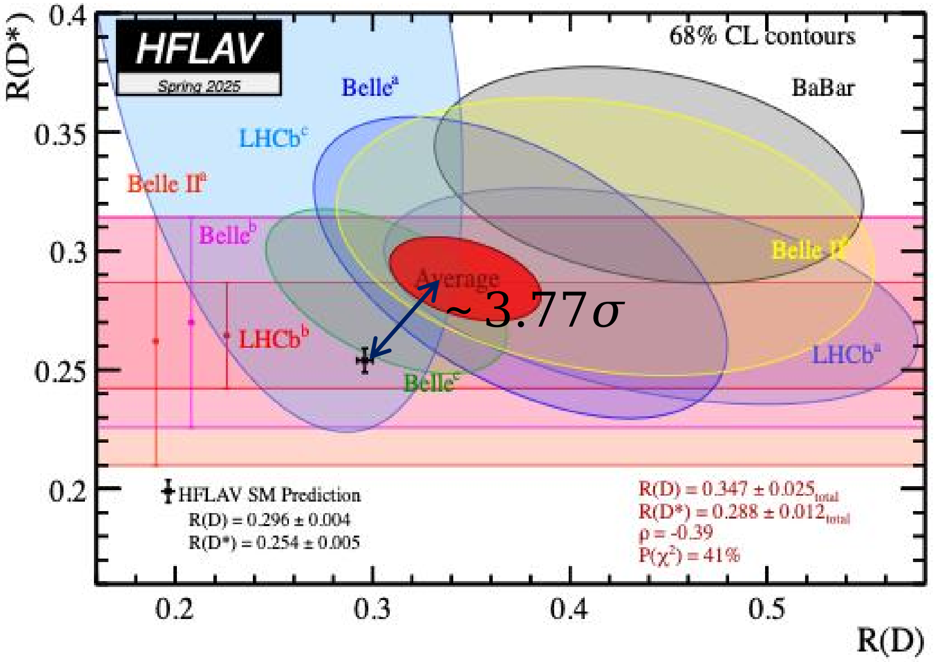

Status

- **We are doing analysis of $\boldsymbol{R(D^*)}$ and $\boldsymbol{R(D)}$ with hadronic tag**

The $R(D^*)$ have been measured with hadronic tagging method use 198 fb^{-1} data

$$R(D^*) = 0.262^{+0.041}_{-0.039}(\mathrm{stat})^{+0.035}_{-0.032}(\mathrm{syst})$$ [Phys. Rev. D 110, 072020]

- **In this time, we measure both the $\boldsymbol{R(D^*)}$ and $\boldsymbol{R(D)}$ use 365 $\boldsymbol{\mathrm{fb}^{-1}}$**

- **CWR1 is on-going**

- **Lastest note**

Reconstruction

- One of B mesons is fully reconstructed with hadronic decays, through the Full Event Interpretation (FEI).

- Exclusive hadronic tagging method :
  Efficiencies B^0: 0.23%, B^+: 0.30%
  arXiv:2008.06096

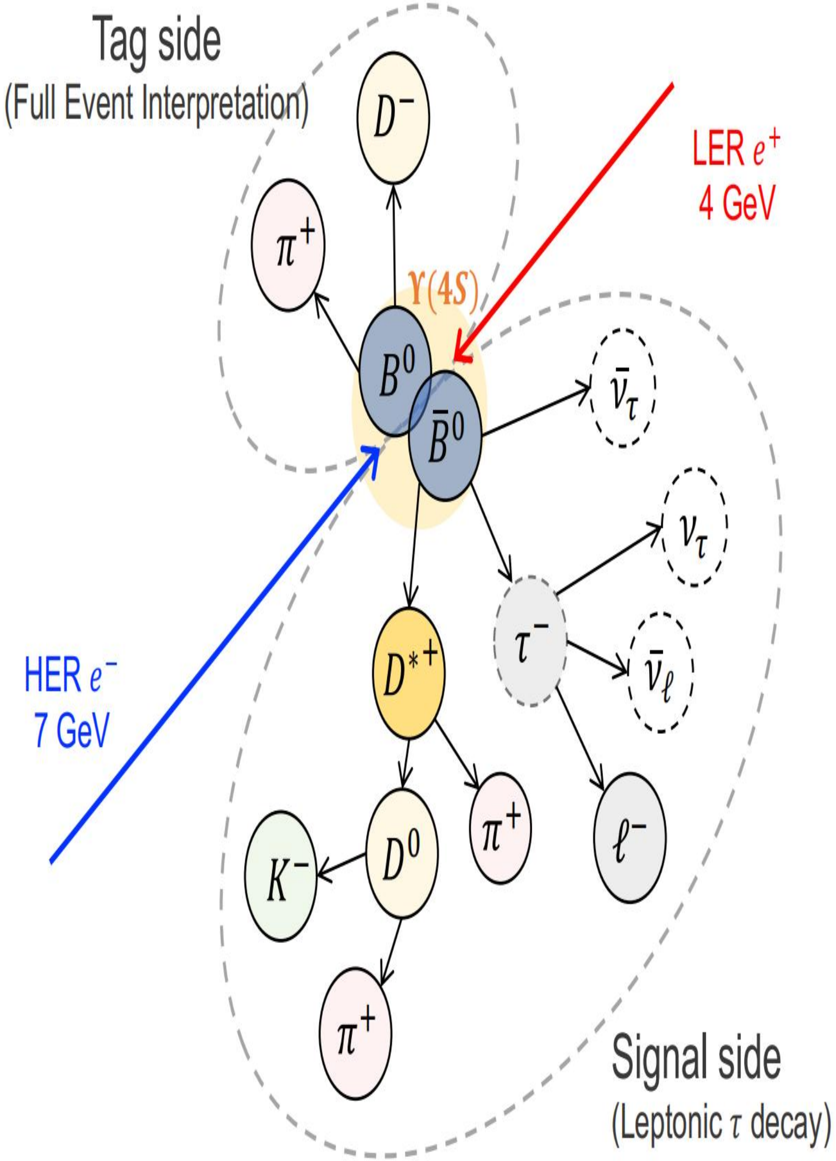

- Reconstructed B decay modes:

$B^0 \,{-}{>}\, D^+\tau^-(\ell^-)\bar{\nu}_{\tau^-(\ell^-)}$

$B^- \,{-}{>}\, D^0\tau^-(\ell^-)\bar{\nu}_{\tau^-(\ell^-)}$

$B^0 \,{-}{>}\, D^{*+}(\,{-}{>}\, D^0\pi^+)\tau^-(\ell^-)\bar{\nu}_{\tau^-(\ell^-)}$

$B^0 \,{-}{>}\, D^{*+}(\,{-}{>}\, D^+\pi^0)\tau^-(\ell^-)\bar{\nu}_{\tau^-(\ell^-)}$

$B^0 \,{-}{>}\, D^{*0}(\,{-}{>}\, D^0\pi^0)\tau^-(\ell^-)\bar{\nu}_{\tau^-(\ell^-)}$

$B^0 \,{-}{>}\, D^{*0}(\,{-}{>}\, D^0\gamma)\tau^-(\ell^-)\bar{\nu}_{\tau^-(\ell^-)}$

- 2D Fitting to extract $R(D^{(*)})$

$$E_{\text{extra}}^{\text{ECL}} = \sum_i E_i^\gamma$$

$$M_{\text{miss}}^2 = (P_{\text{beam}} - P_B - P_{D^{(*)}} - P_\ell)^2$$

Data and Correction

- Data: 365fb-1, proc13+prompt
- MC15rd:

  generic BB, continuum(cuds) 1444fb-1

  BG MC of D**lν, gap mode
- Several corrections are applied to data and MC, in order to improve data/MC agreement
- Correction factors are applied following performance recommendation

  track momentum scale (tracking_data_Moriond23_v1)

  photon energy bias correction (PhotonEnergyBiasCorrection_MC15rd_June2023)

  (applied for data)

  hadron, lepton PID (leptonid_official_rel6_mc15rd)

  slow $\pi^{\pm}$ efficiency (provided by tracking group)

  γ efficiency (PhotonEfficiencyDataMCRatio_Run1MC15rd_April2024)

  π^{0} efficiency (provided by neutral group locally by using our π^{0} selection)

  mode dependent FEI efficiency (provided by provided group)

  form factor correction (following WG1 recommendation)

  D^{**} branching retion correction (following WG1 recommendatiom)

  B hadronic decay branching ration (following PDG)

  (applied for MC)

Selection: B_{tag}

- B_{tag} selection criteria is the same as FEI calibration analysis of $B \to X\ell\nu$ and $B \to D^{(*)}\pi$

variable	selection criteria
event	nCleanedTrack > 4
B_{tag}	$p_{\mathrm{FEI}} > 0.01$, $M_{\mathrm{bc}} > 5.27$ GeV, $-0.15 < \Delta E < 0.1$ GeV, $cos\theta_{\mathrm{TBTO}} < 0.9$

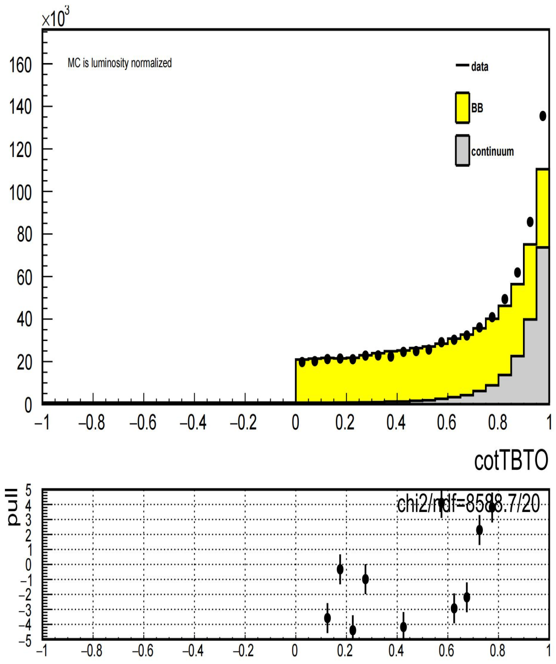

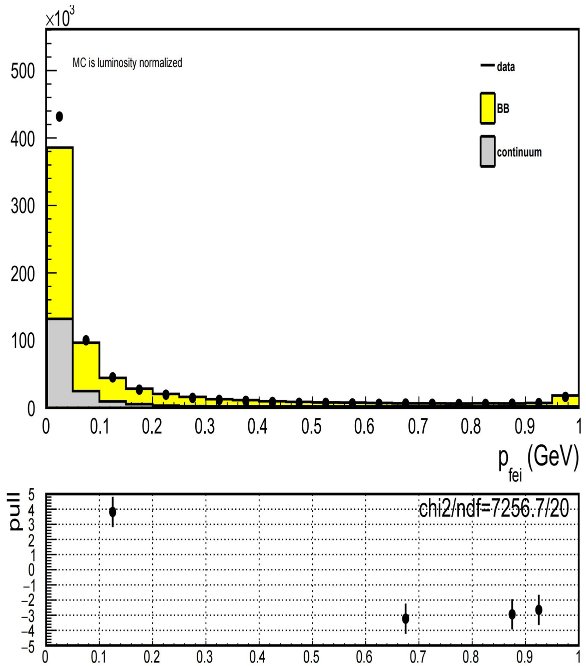

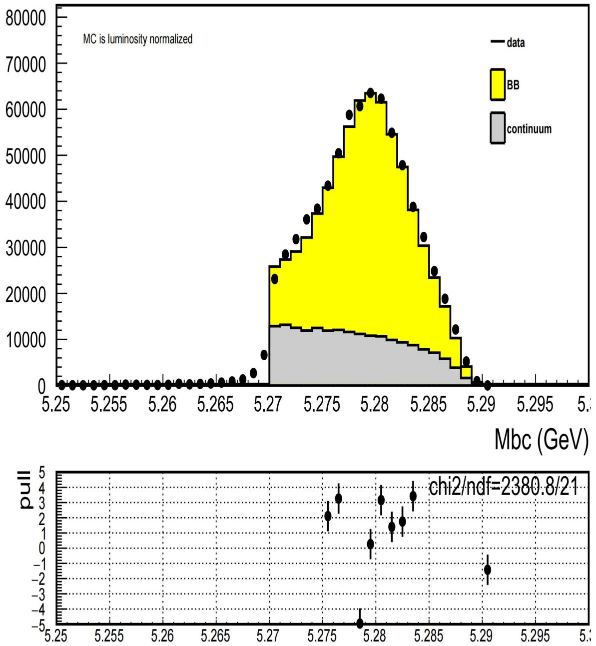

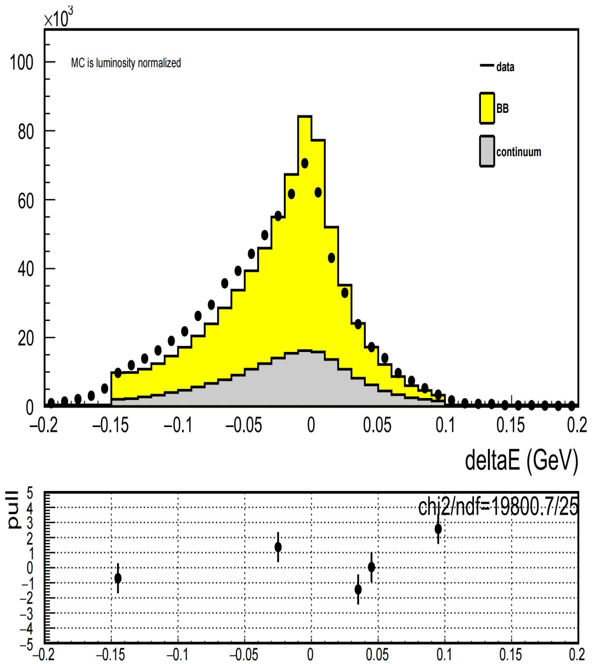

Selection: $B_{\mathbf{sig}}$

K, π
- nCDCHits is removed to increase statistics ($+\sim30\%$ stat.)
- reject low K: fake rate correction is not available on systematic framework ($-\sim10\%$ stat.)

e, μ
- $p > 0.4\ (0.7)$ GeV is applied for PID, reach ECL(KLM) ($-\sim20\%$ stat.)
- BremsCorrection is added to electron

K_S
- distance cut is removed because data/MC looks no problem ($+\sim5\%$ stat.)

B_{sig}	selection
charged track	$\mathrm{d}r < 2$ cm, $\lvert\mathrm{d}z\rvert < 4$ cm
π	good track, $P_{\pi}^{binary} > 0.1$ or $p < 0.3$ GeV, $p_{\mathrm{T}} > 0.1$ GeV/c
K	good track, $P_{K}^{binary} > 0.1$ and $p > 0.3$ GeV, $p_{\mathrm{T}} > 0.1$ GeV/c
π_{slow}	$p > 0.05$ GeV/c
K_{S}	KsSelector "standard"
π^0	pi0:eff40_May2020, γ: $\lvert$clusterTiming$\rvert < 200$ ns, $122.4 < M < 143.0$ GeV, combination of minC2TDist and zernikeMVA
π^0_{slow}	pi0:eff50_May2020, γ: $\lvert$clusterTiming$\rvert < 200$ ns, $118.3 < M < 147.0$ MeV, combination of minC2TDist and zernikeMVA, $p > 0.05$GeV
e	$p > 0.4$ GeV, $P_e^{\text{global}} > 0.9$(BDT), Bremss correction
μ	$p > 0.7$ GeV, $P_\mu^{\text{global}} > 0.9$(likelihood)
$D,\ D^*$	mode dependent D mass, $D^* - D$ mass difference cut
B_{sig}	$q^2 > 4\ \mathrm{GeV}^2$

Selection: ROE

- γ energy is increased to 100(FW), 50(BR), 100(BW) for better data/MC
- photon MVA variables(fakePhotonSuppressionMVA, beamBackgroundSuppressionMVA) are added to reject fake photons and beambbackgroud
- π^0 veto is enhanced to reduce $D^{**}\ell\nu$, hadron BG

ROE	selection criteria	
ROE mask	Tracks	$dr < 2$ cm, $\lvert dz \rvert < 4$ cm, $p_{\mathrm{T}} > 0.1$ GeV/c, nCDCHits > 0
	Clusters	energy > 0.08(FW), 0.05(BR), 0.06(BW), |clusterTiming| < 200 ns minC2TDist > 15 cm, fakePhotonSuppressionMVA > 0.2, beamBackgroundSuppressionMVA > 0.5
Charged track	nROE_Tracks < 1	
Neutral cluster	$N(\pi^0) < 1$ with eff30	

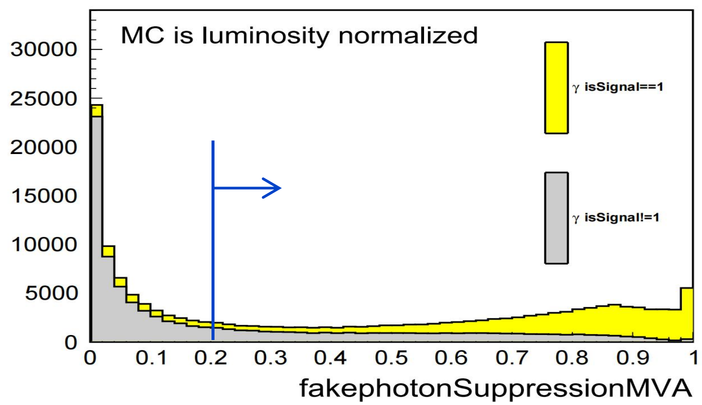

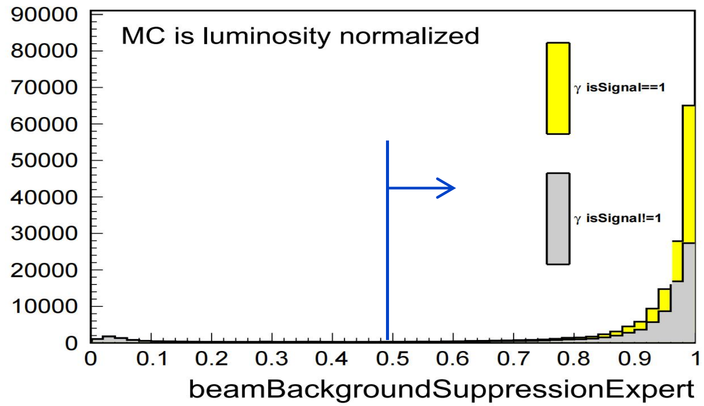

Selected events

- Expected yields of candidate categories and $D^{(*)}$ modes at 363fb^{-1} in MC after all selections. The SM $R(D^*)$ value at 0.254, and the $R(D)$ at 0.30.
- ~600(300) $\bar{B} \to D^*\tau^-\bar{\nu}_\tau$ ($\bar{B} \to D\tau^-\bar{\nu}_\tau$) events are expected.

Table 3.11: Expected yields of candidate categories and D^* modes at 365 fb^{-1} in MC after all selections. The world average $R(D^{(*)})$ values are assumed for yields of $\overline{B} \to D^*\tau^-\overline{\nu}_\tau$.

Category	Expected yields in MC					
	$D^{*+} \to D^0\pi^+$	$D^{*+} \to D^+\pi^0$	$D^{*0} \to D^0\pi^0$	$D^{*0} \to D^0\gamma$	D^0	D^+
$B \to D^*\tau\nu$	107	14	63	104	372	61
$B \to D\tau\nu$	0	0	1.4	21	240	101
$B \to D^*\ell\nu$	2366	294	1306	2379	9788	1478
$B \to D\ell\nu$	0.9	2.9	6.9	216	2920	1229
$B \to D^{**}\ell\nu, D^{**}\tau\nu$ and gap	196	37	120	442	1583	557
hadronic B decay	86	14	44	162	605	279
continuum	2.1	0.8	2.2	33	181	84
others	0.2	0	0	0.1	0.8	4.2
Total	2758	360	1543	3358	15686	3793

Selected events: $M^2_{\mathbf{miss}}$

- MC distribution of M^2_{miss} for each $D^{(*)}$ decay mode in each $D^{(*)}$ decay mode

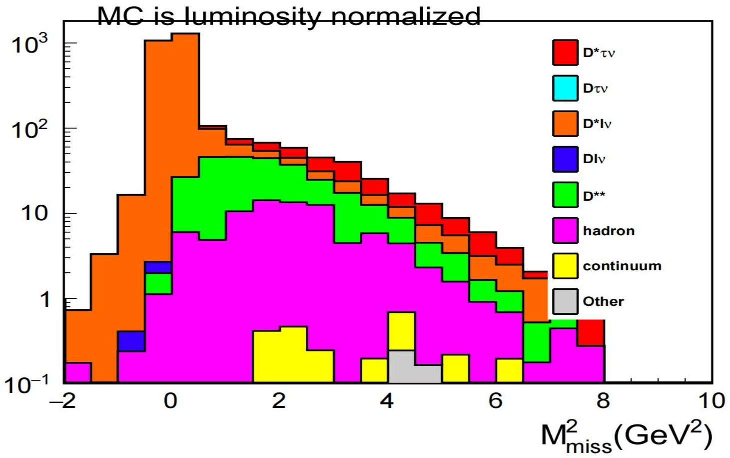

$(a) B^0 \text{ -> } \mathrm{D}^{*+}\tau^-\bar{\nu}_{\tau^-}(\mathrm{D}^{*+} \text{ -> } \mathrm{D}^0\pi^+)$

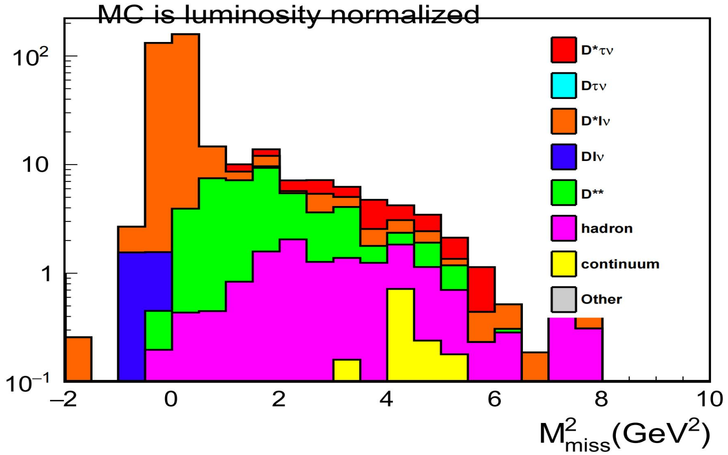

$(b) B^0 \text{ -> } \mathrm{D}^{*+}\tau^-\bar{\nu}_{\tau^-}(\mathrm{D}^{*+} \text{ -> } \mathrm{D}^+\pi^0)$

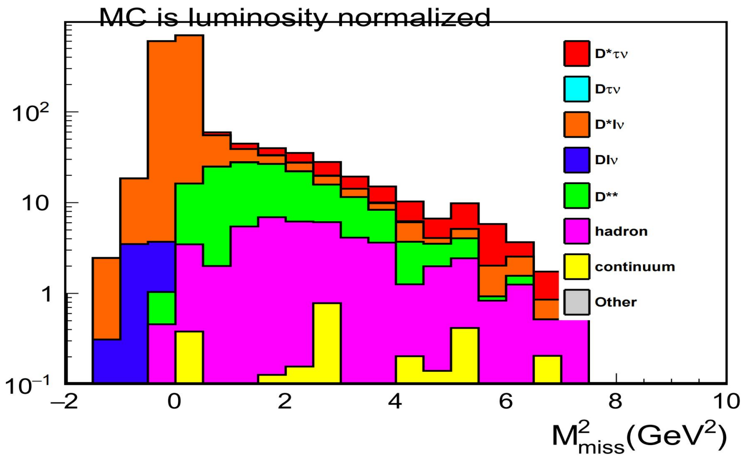

$(c) B^- \text{ -> } \mathrm{D}^{*0}\tau^-\bar{\nu}_{\tau^-}(\mathrm{D}^{*0} \text{ -> } \mathrm{D}^0\pi^0)$

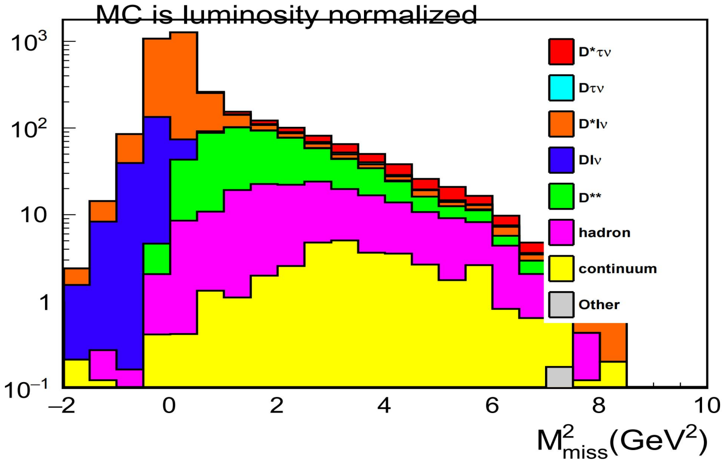

$(d) B^- \text{ -> } \mathrm{D}^{*0}\tau^-\bar{\nu}_{\tau^-}(\mathrm{D}^{*0} \text{ -> } \mathrm{D}^0\gamma^0)$

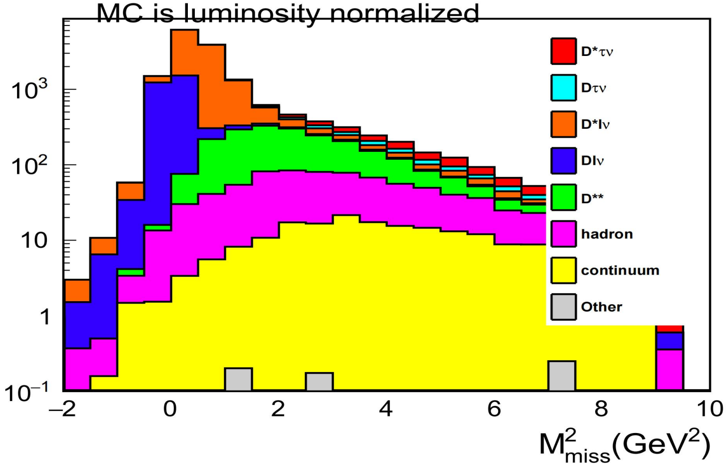

$(e) B^- \text{ -> } \mathrm{D}^0\tau^-\bar{\nu}_{\tau^-}$

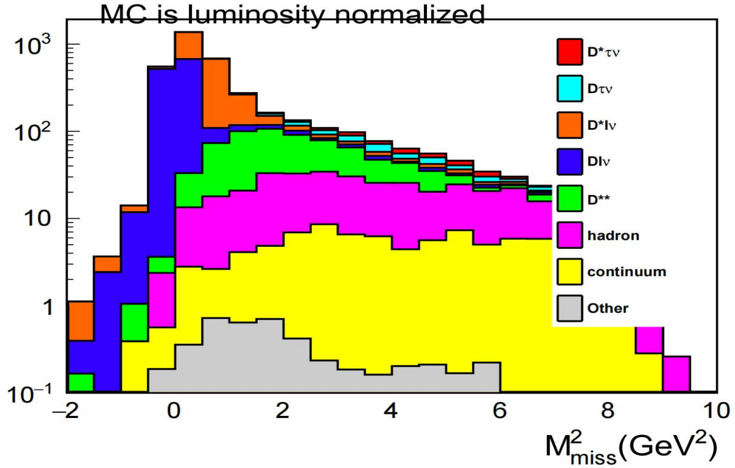

$(f) B^0 \text{ -> } \mathrm{D}^+\tau^-\bar{\nu}_{\tau^-}$

Selected events: E_{extra}^{ECL}

- MC distribution of $E_{\mathrm{extra}}^{\mathrm{ECL}}$ for each $D^{(*)}$ decay mode

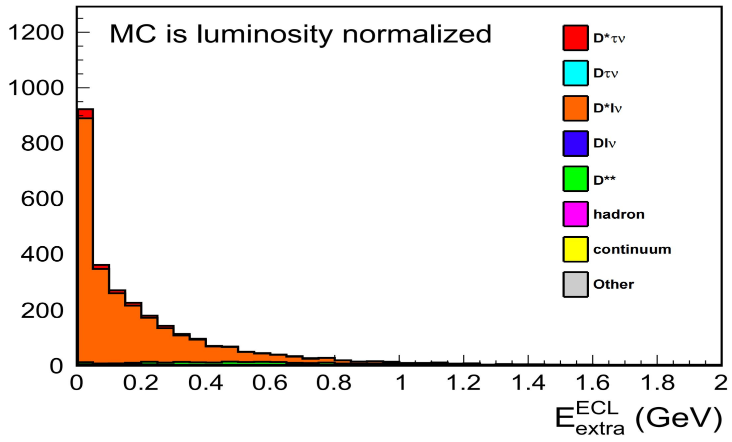

$(a) B^0 \rightarrow D^{*+}\tau^-\bar{\nu}_{\tau^-} (D^{*+} \rightarrow D^0\pi^+)$

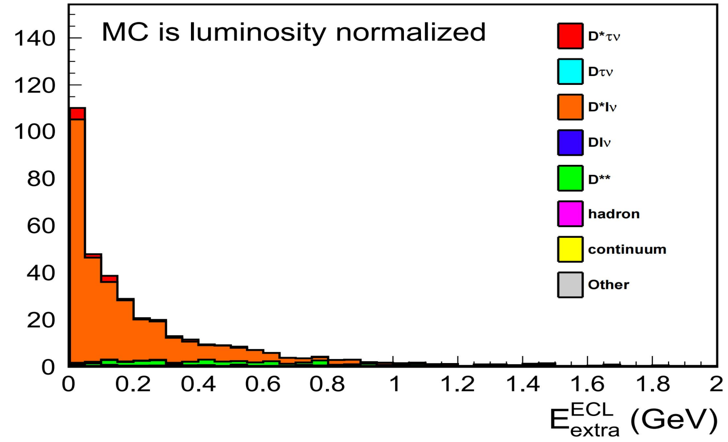

$(b) B^0 \rightarrow D^{*+}\tau^-\bar{\nu}_{\tau^-} (D^{*+} \rightarrow D^+\pi^0)$

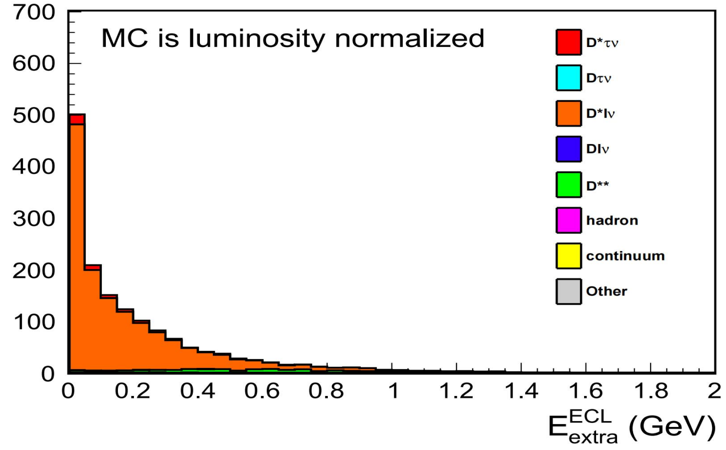

$(c) B^- \rightarrow D^{*0}\tau^-\bar{\nu}_{\tau^-} (D^{*0} \rightarrow D^0\pi^0)$

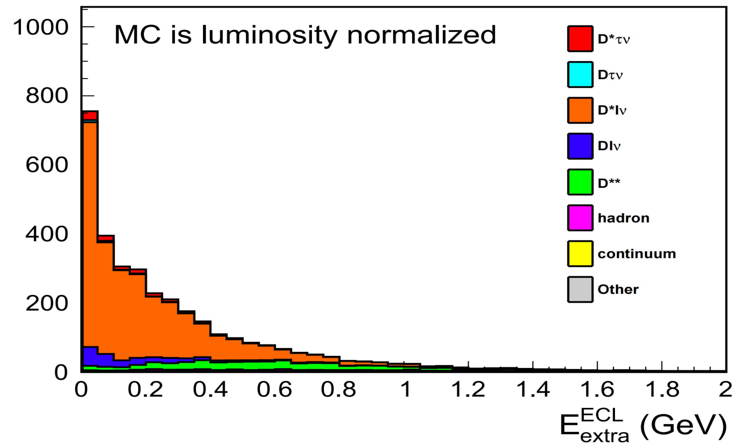

$(d) B^- \rightarrow D^{*0}\tau^-\bar{\nu}_{\tau^-} (D^{*0} \rightarrow D^0\gamma^0)$

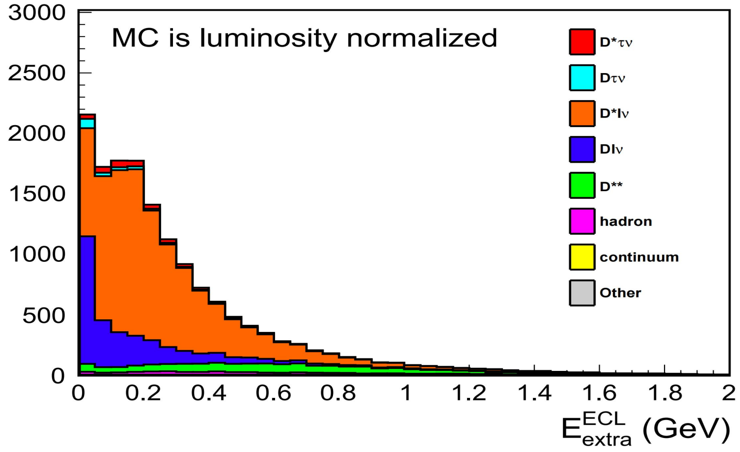

$(e) B^- \rightarrow D^0\tau^-\bar{\nu}_{\tau^-}$

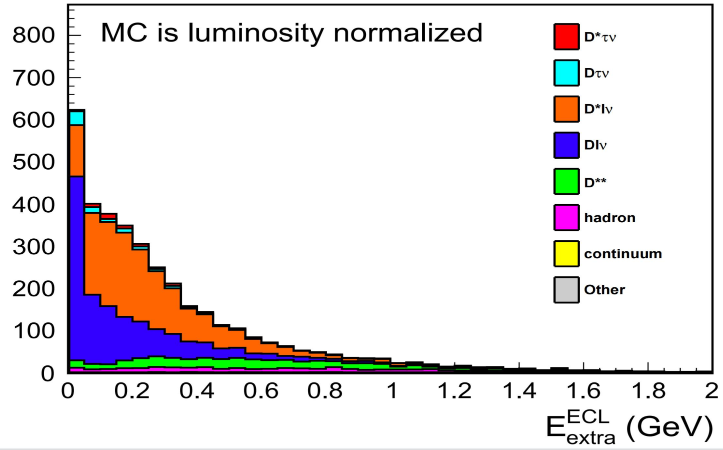

$(f) B^0 \rightarrow D^+\tau^-\bar{\nu}_{\tau^-}$

Selected events: $\mathbf{E_{extra}^{ECL}}$

- MC distribution of $E_{\mathrm{extra}}^{\mathrm{ECL}}$ for each $D^{(*)}$ decay mode with high missing mass squire cut(1.5<$E_{\mathrm{extra}}^{\mathrm{ECL}}$<6.0 for D^{*} and 3.0<$E_{\mathrm{extra}}^{\mathrm{ECL}}$<8.0 for D)

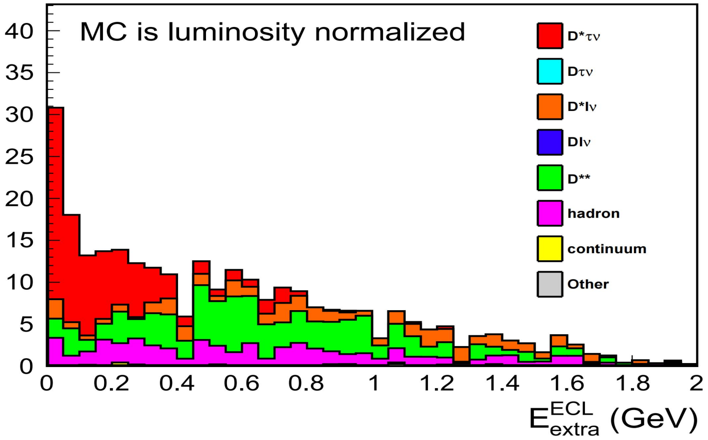

$(a) B^0$ —> $\mathrm{D}^{*+}\tau^-\bar{\nu}_{\tau^-}$($\mathrm{D}^{*+}$ —> $\mathrm{D}^0\pi^+$)

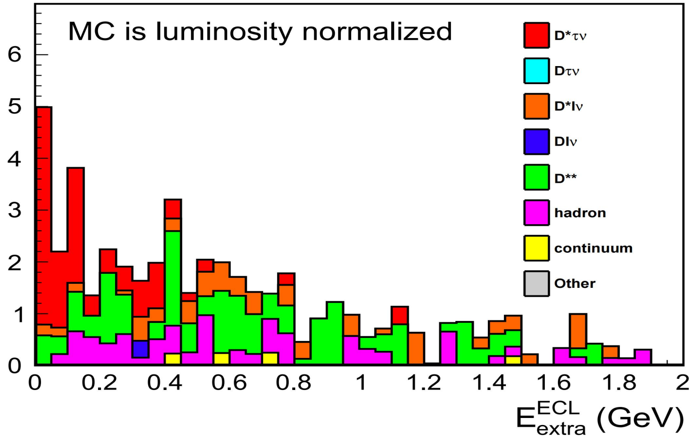

$(b) B^0$ —> $\mathrm{D}^{*+}\tau^-\bar{\nu}_{\tau^-}$($\mathrm{D}^{*+}$ —> $\mathrm{D}^+\pi^0$)

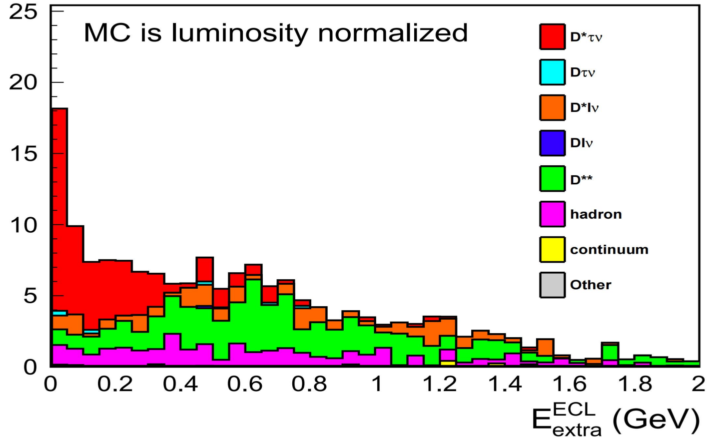

$(c) B^-$ —> $\mathrm{D}^{*0}\tau^-\bar{\nu}_{\tau^-}$($\mathrm{D}^{*0}$ —> $\mathrm{D}^0\pi^0$)

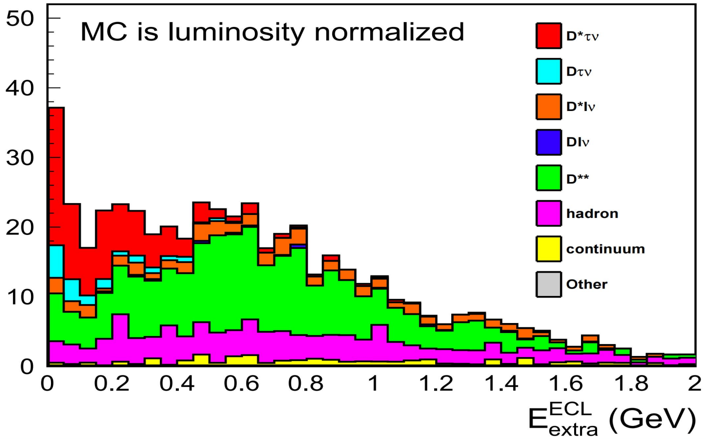

$(d) B^-$ —> $\mathrm{D}^{*0}\tau^-\bar{\nu}_{\tau^-}$($\mathrm{D}^{*0}$ —> $\mathrm{D}^0\gamma^0$)

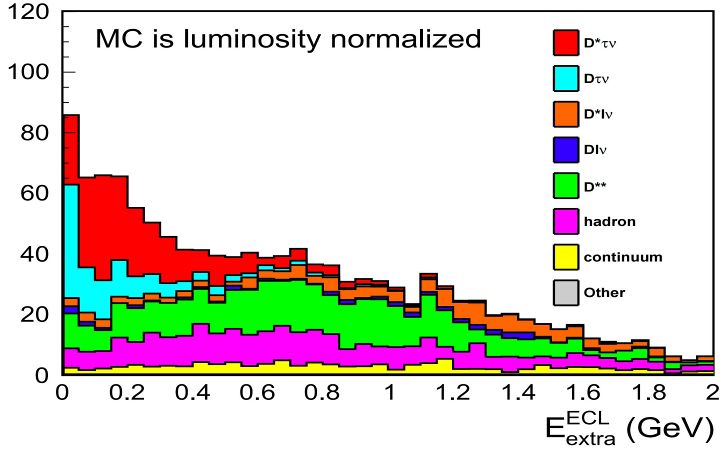

$(e) B^-$ —> $\mathrm{D}^0\tau^-\bar{\nu}_{\tau^-}$

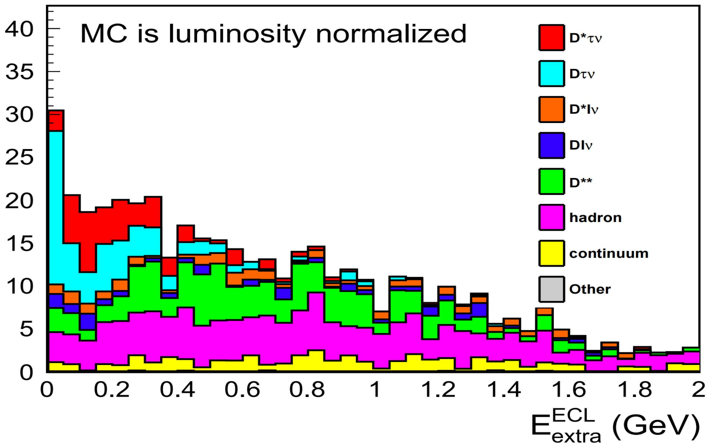

$(f) B^0$ —> $\mathrm{D}^+\tau^-\bar{\nu}_{\tau^-}$

Data/MC agreement at sideband

- Summary of sideband regions used to check Data/MC agreement

sidebane	selection	enhanced mode	ckeck item
q^2 sideband	$q^2 < 3.5\ \mathrm{GeV}^2$	$B -> D^{(*)}\ell\upsilon$	signal effieincy signal PDF
π^0 veto sideband	$N_{\pi^0\mathrm{ROE}} > 0$	$B -> D^{**}\ell\upsilon$	BG yield BG PDF
	$E_{\mathrm{ECL}}^{\mathrm{extra}} > 1\ \mathrm{GeV}$	hadronic BG	
	$M_{\mathrm{miss}}^2 > 2\ \mathrm{GeV}$	continuum BG	

q^2 sideband

- Data/MC comparison of the number of elected events at q^2 sideband

Table 5.2: Data/MC comparison of the number of selected events in the q^2 side-band. The error shows statistical error of data. systematic error is not included in the error.

Category	The number of selected events)					
	$D^{*+} \to D^0\pi^+$	$D^{*+} \to D^+\pi^0$	$D^{*0} \to D^0\pi^0$	$D^{*0} \to D^0\gamma$	D^0	D^+
Data	1422	144	712	1481	5585	1988
Total MC	1432	170	707	1476	5443	1928
Data/MC ratio	0.993	0.848	1.007	1.004	1.026	1.032
(stat. error)	± 0.026	± 0.071	± 0.038	± 0.026	± 0.014	± 0.023

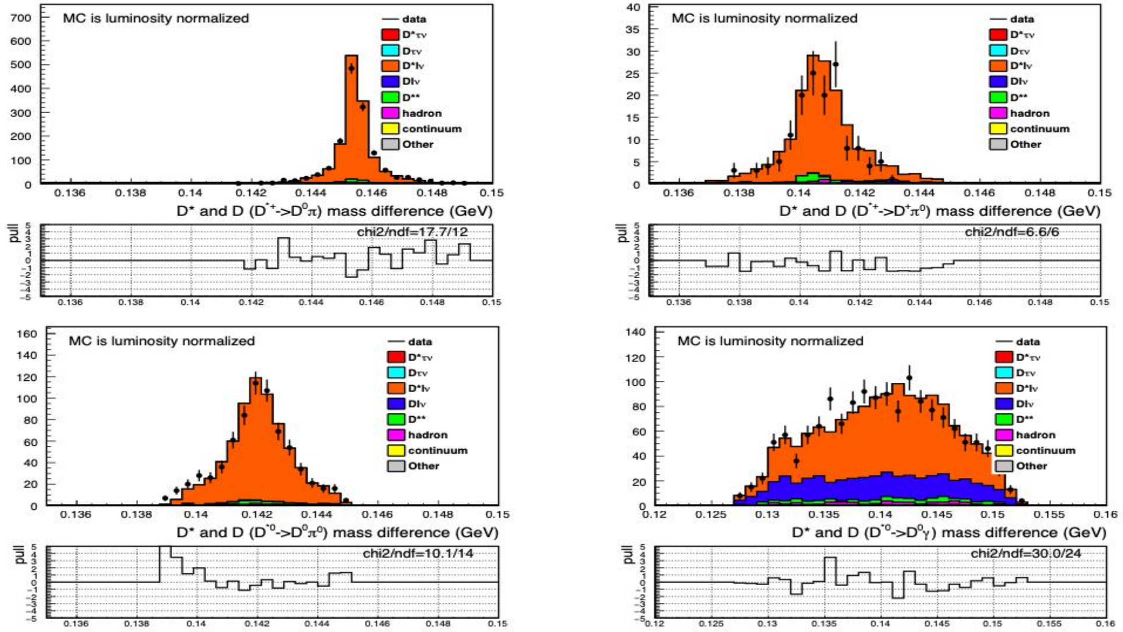

Data yield is lower at $D^+ \to K^-\pi^+\pi^-\pi^0$ and $D^+ \to K^0_S\pi^+\pi^0$, $D^0 \to K^-K^+$, $D^0 \to K^-\pi^+\pi^-\pi^+$ related D^+ decay, the difference is taken as systematic error.

q^2 sideband: $\mathbf{E}_{\mathbf{extra}}^{\mathbf{ECL}}$

- Distributions of the $E_{\mathrm{extra}}^{\mathrm{ECL}}$ in each $D^{(*)}$ decay mode at q2 sideband

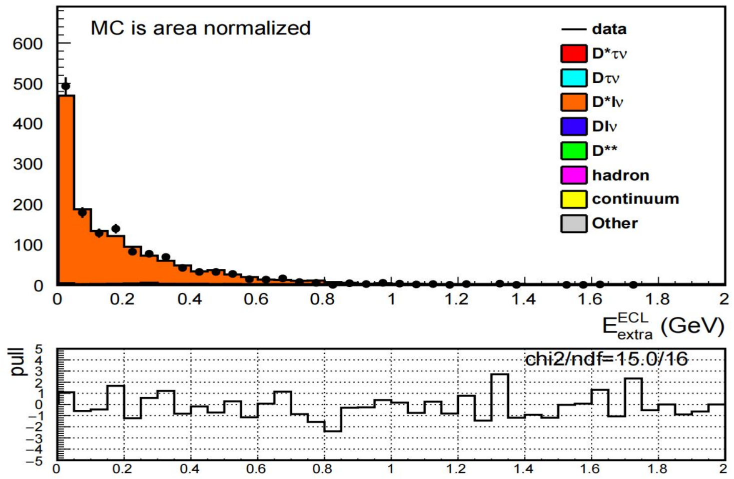

$(a) B^0 -> \mathrm{D}^{*+}\tau^-\bar{\nu}_{\tau^-}(\mathrm{D}^{*+} -> \mathrm{D}^0\pi^+)$

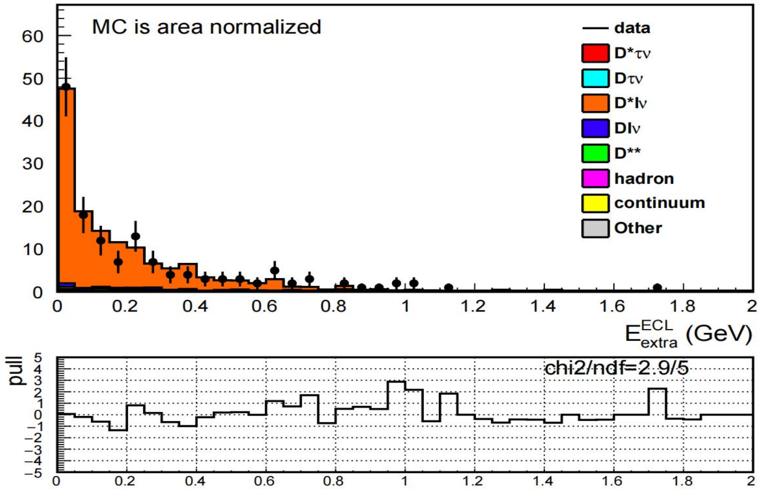

$(b) B^0 -> \mathrm{D}^{*+}\tau^-\bar{\nu}_{\tau^-}(\mathrm{D}^{*+} -> \mathrm{D}^+\pi^0)$

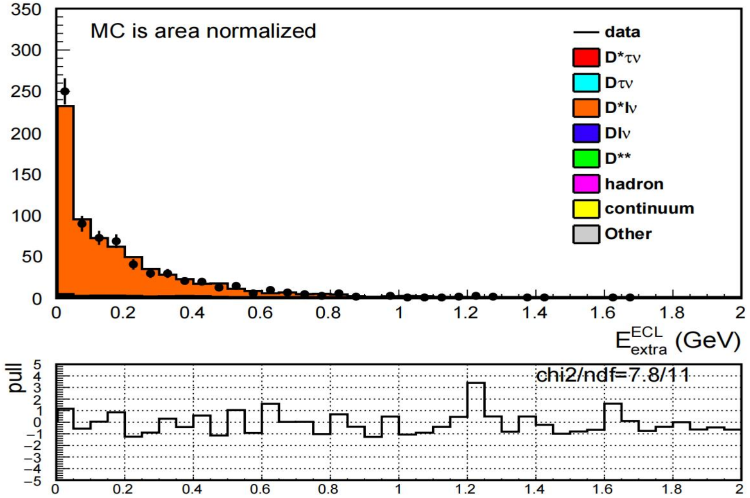

$(c) B^- -> \mathrm{D}^{*0}\tau^-\bar{\nu}_{\tau^-}(\mathrm{D}^{*0} -> \mathrm{D}^0\pi^0)$

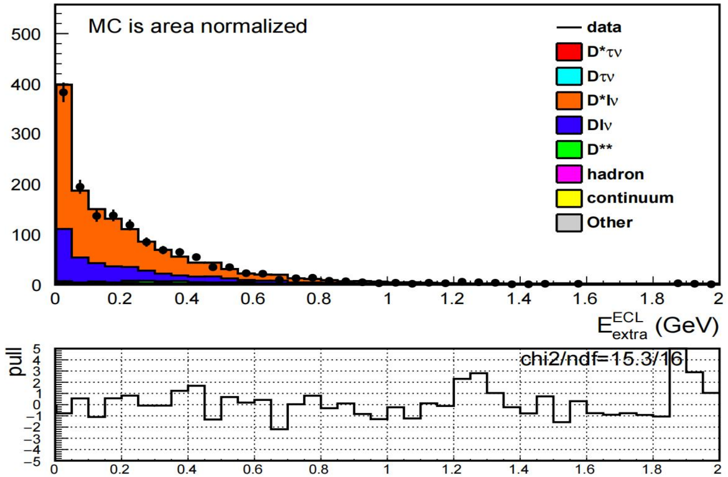

$(d) B^- -> \mathrm{D}^{*0}\tau^-\bar{\nu}_{\tau^-}(\mathrm{D}^{*0} -> \mathrm{D}^0\gamma^0)$

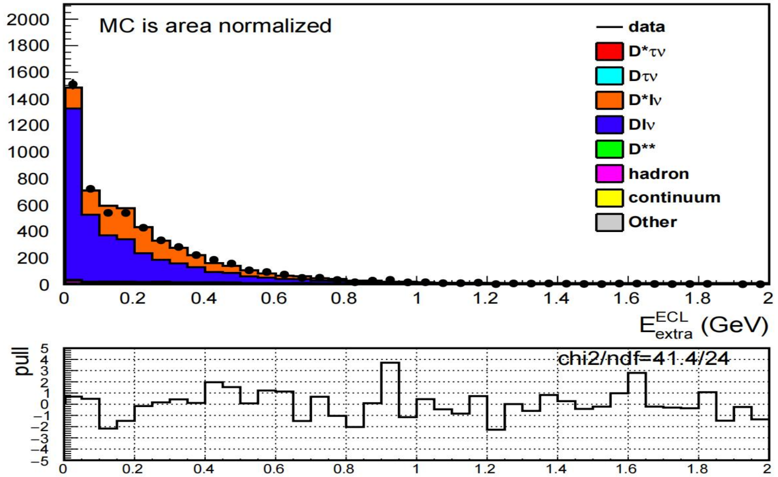

$(e) B^- -> \mathrm{D}^0\tau^-\bar{\nu}_{\tau^-}$

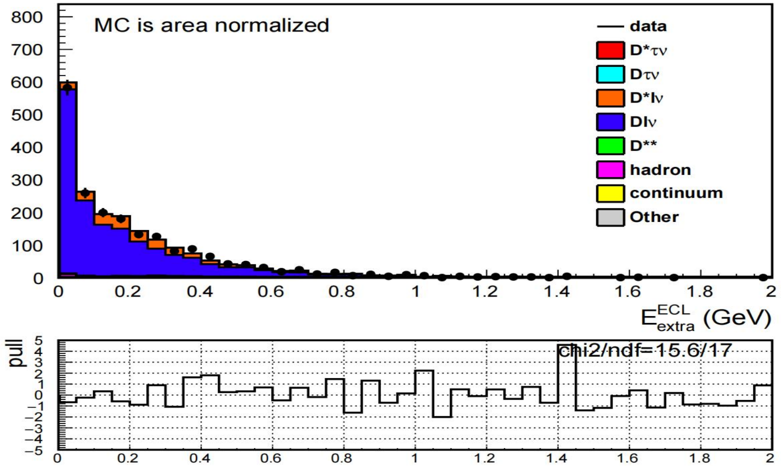

$(f) B^0 -> \mathrm{D}^+\tau^-\bar{\nu}_{\tau^-}$

q^2 sideband: M^2_{miss}

- Distributions of the M^2_{miss} in each $D^{(*)}$ decay mode at q2 sideband

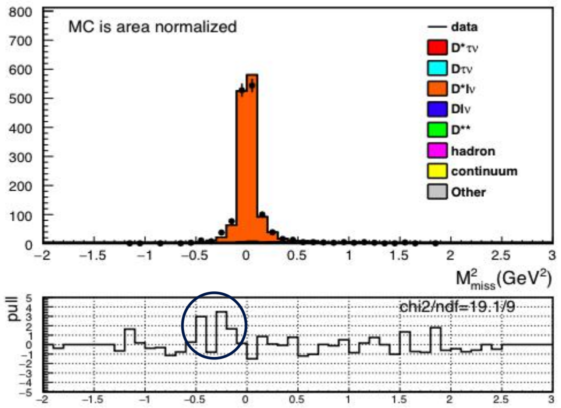

$(a) B^0 \rightarrow D^{*+}\tau^-\bar{\nu}_{\tau^-} (D^{*+} \rightarrow D^0\pi^+)$

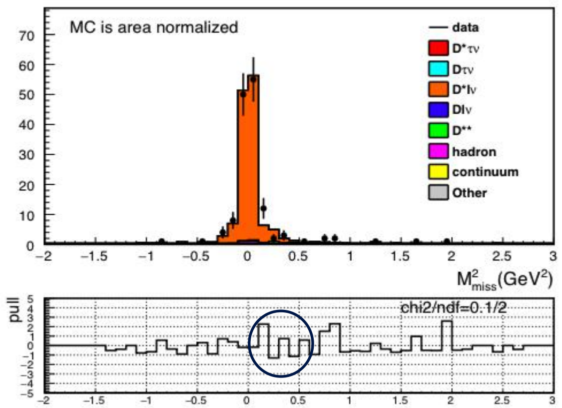

$(b) B^0 \rightarrow D^{*+}\tau^-\bar{\nu}_{\tau^-} (D^{*+} \rightarrow D^+\pi^0)$

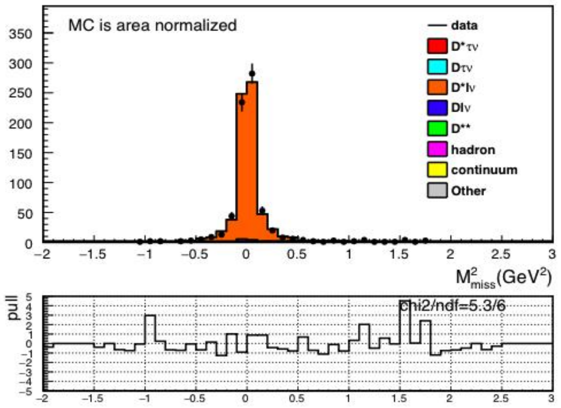

$(c) B^- \rightarrow D^{*0}\tau^-\bar{\nu}_{\tau^-} (D^{*0} \rightarrow D^0\pi^0)$

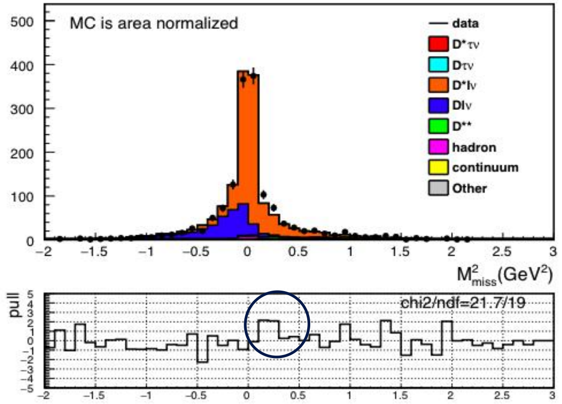

$(d) B^- \rightarrow D^{*0}\tau^-\bar{\nu}_{\tau^-} (D^{*0} \rightarrow D^0\gamma^0)$

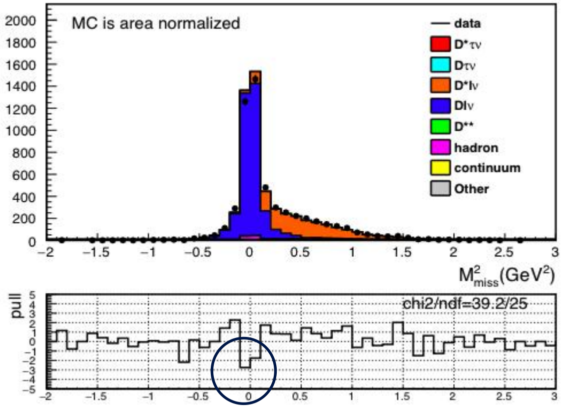

$(e) B^- \rightarrow D^0\tau^-\bar{\nu}_{\tau^-}$

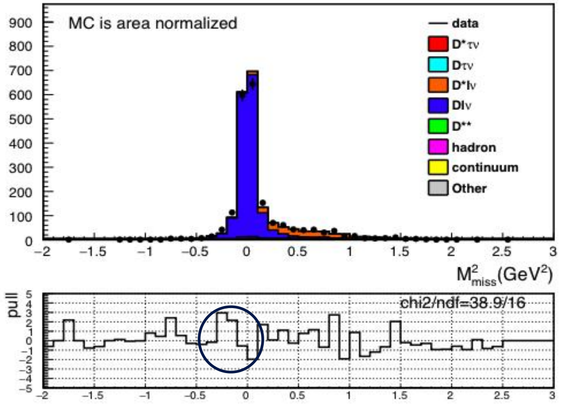

$(f) B^0 \rightarrow D^+\tau^-\bar{\nu}_{\tau^-}$

- Good data/MC but their resolution is slightly different
- Data/MC ratio of M^2_{miss} width is estimated by fitting, MC is smeared by using the ratio

D decay	$\Delta\sigma$ (GeV^2)
D^{*+}	0.0398±0.0037
$D^{*0} \to D^0\pi^0$	0.0249±0.0129
$D^{*0} \to D^0\gamma$	0.0472±0.0070
D^0	0.0399±0.0098
D^+	0.0450±0.0070

π^0 veto sideband

- Data/MC comparison of the number of elected events at π^0 veto sideband, and the data yield is 10-40% smaller than MC expectation in each sample
- In order to investigate this issue, new MC category of ”un-measured hadronic B decay” and ”$D^{**}\ell\nu$ gap mode” are added

Table 5.5: Data/MC comparison of the number of selected events in the π^0 veto sideband. The error shows statistical error of data.

Category	The number of selected events					
	$D^{*+} \to D^0\pi^+$	$D^{*+} \to D^+\pi^0$	$D^{*0} \to D^0\pi^0$	$D^{*0} \to D^0\gamma$	D^0	D^+
Data	85	24	49	397	1421	764
(± stat.)	± 9	± 5	± 7	± 20	± 38	± 28
MC $B \to D^{**}\ell\nu$, gap mode	22	3.1	19	79	354	131
MC hadronic B decay, unmeasured BR	28	11	17	90	287	293
MC $B \to D^{**}\ell\nu$, non-gap mode	13	1.4	9.9	34	191	78
MC hadronic B decay, measured BR	34	11	31	124	420	215
MC continuum	5.5	3.6	5.5	67	348	199
MC others, $B \to D^{(*)}\ell\nu$	10.4	1.5	4.4	15	118	30
MC Total	116	31.7	86.9	408.8	1718	946
(± 100% error of unmeasured BR)	± 22 ± 28	± 3.1 ± 11	± 19 ± 17	± 79 ± 90	± 354 ± 287	± 131 ± 293
Data/MC (stat.)	0.75 ± 0.08	0.76 ± 0.15	0.56 ± 0.08	0.97 ± 0.05	0.83 ± 0.02	0.81 ± 0.03
(± 100% error of unmeasured BR)	± 0.17 ± 0.25	± 0.09 ± 0.44	± 0.15 ± 0.15	± 0.24 ± 0.28	± 0.22 ± 0.17	± 0.13 ± 0.36

π^0 veto sideband: M^2_{miss}

- Distributions of the M^2_{miss} in each $D^{(*)}$ decay mode at q2 sideband

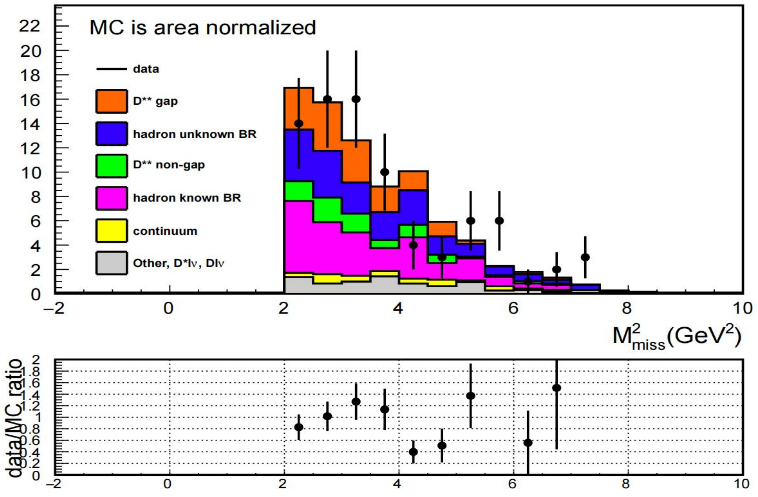

$(a) B^0 -> \mathrm{D}^{*+}\tau^-\bar{\nu}_{\tau^-}(\mathrm{D}^{*+} -> \mathrm{D}^0\pi^+)$

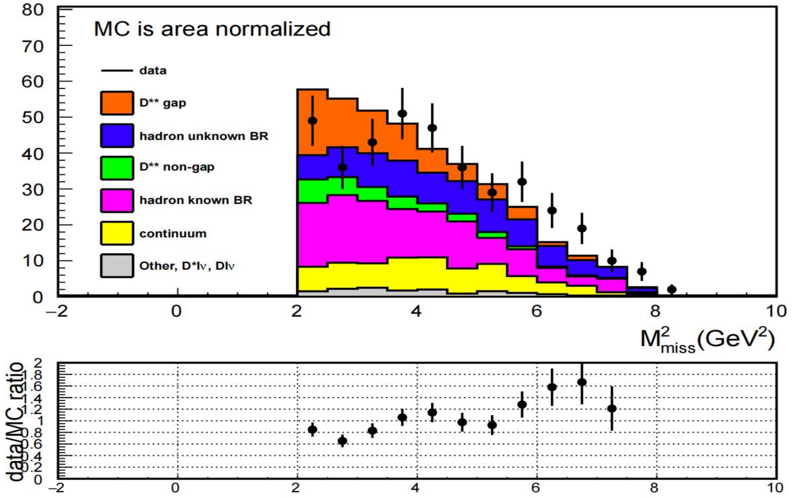

$(b) B^0 -> \mathrm{D}^{*+}\tau^-\bar{\nu}_{\tau^-}(\mathrm{D}^{*+} -> \mathrm{D}^+\pi^0)$

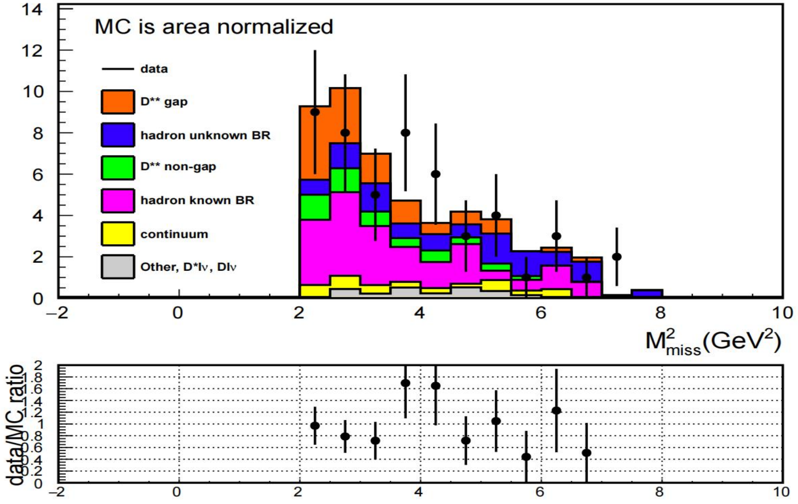

$(c) B^- -> \mathrm{D}^{*0}\tau^-\bar{\nu}_{\tau^-}(\mathrm{D}^{*0} -> \mathrm{D}^0\pi^0)$

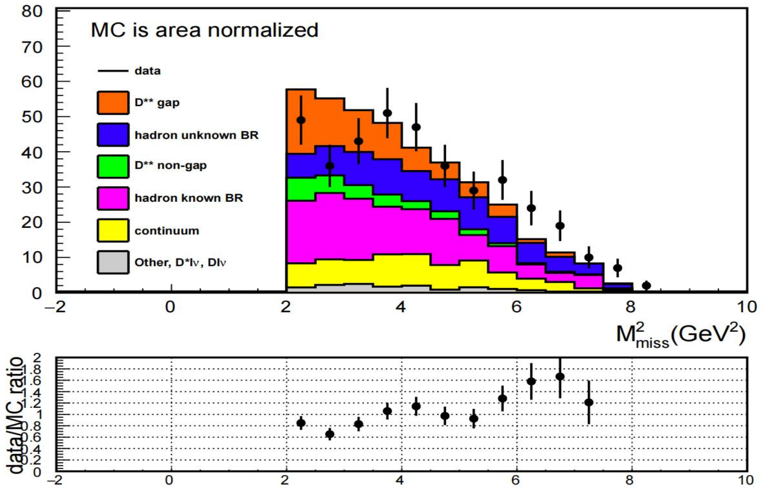

$(d) B^- -> \mathrm{D}^{*0}\tau^-\bar{\nu}_{\tau^-}(\mathrm{D}^{*0} -> \mathrm{D}^0\gamma^0)$

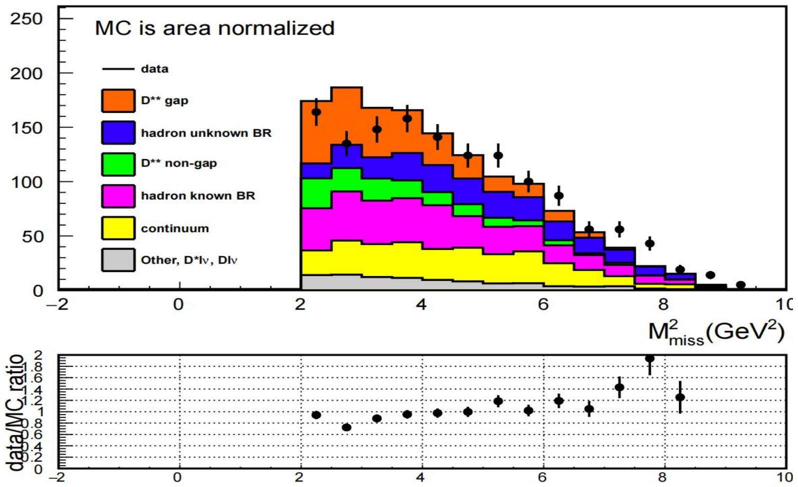

$(e) B^- -> \mathrm{D}^0\tau^-\bar{\nu}_{\tau^-}$

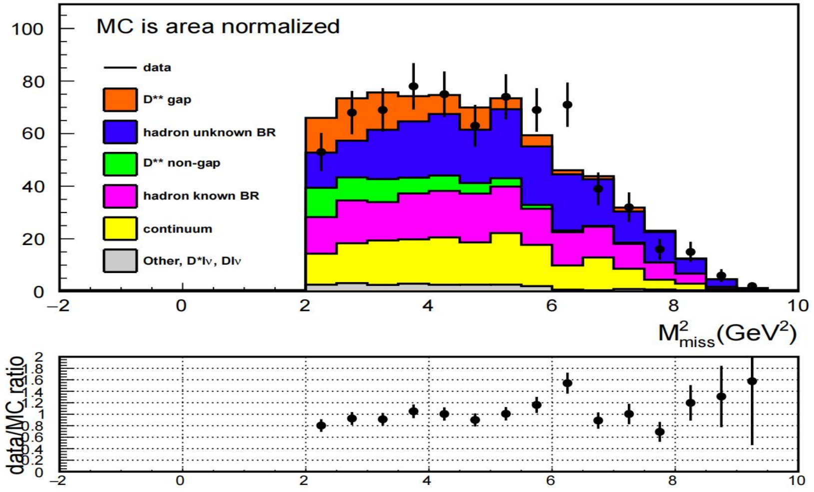

$(f) B^0 -> \mathrm{D}^+\tau^-\bar{\nu}_{\tau^-}$

π^0 veto sideband: $E_{\mathrm{extra}}^{\mathrm{ECL}}$

- Distributions of the $E_{\mathrm{extra}}^{\mathrm{ECL}}$ in each $D^{(*)}$ decay mode at q2 sideband

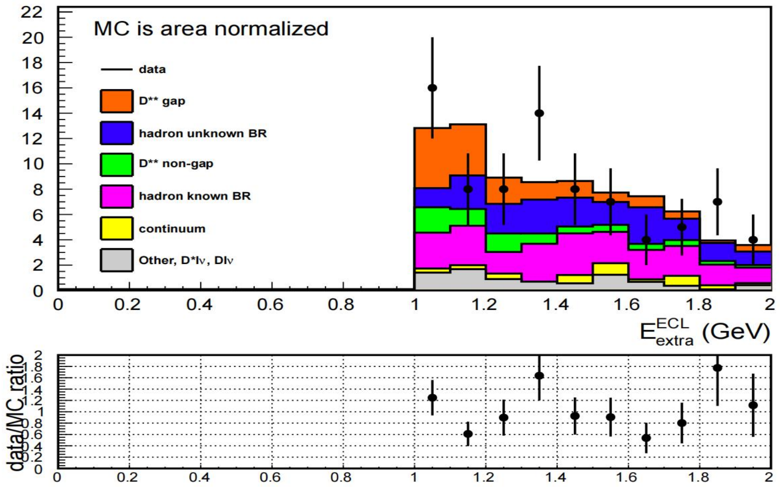

$(a) B^0 \to D^{*+}\tau^-\bar{\nu}_{\tau^-} (D^{*+} \to D^0\pi^+)$

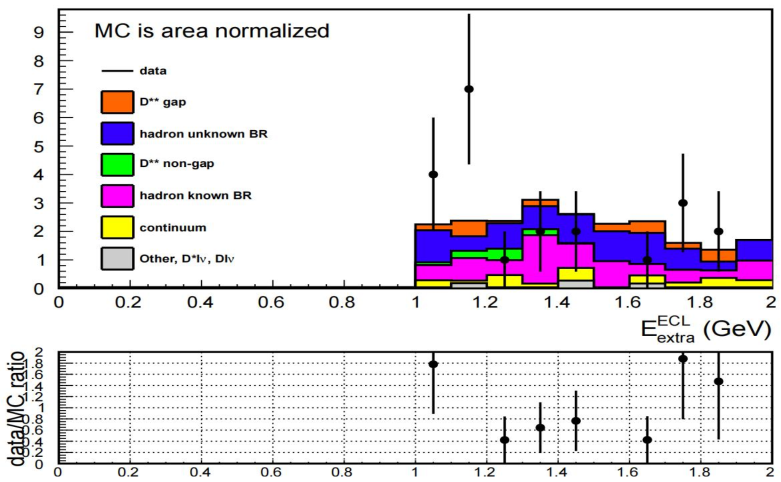

$(b) B^0 \to D^{*+}\tau^-\bar{\nu}_{\tau^-} (D^{*+} \to D^+\pi^0)$

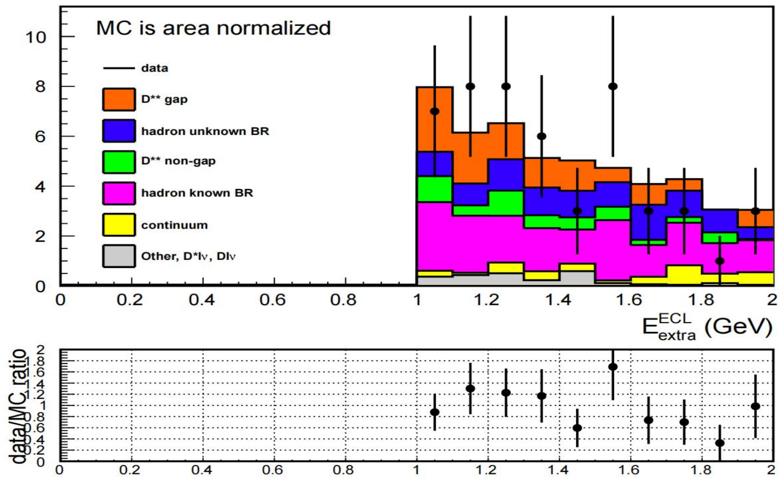

$(c) B^- \to D^{*0}\tau^-\bar{\nu}_{\tau^-} (D^{*0} \to D^0\pi^0)$

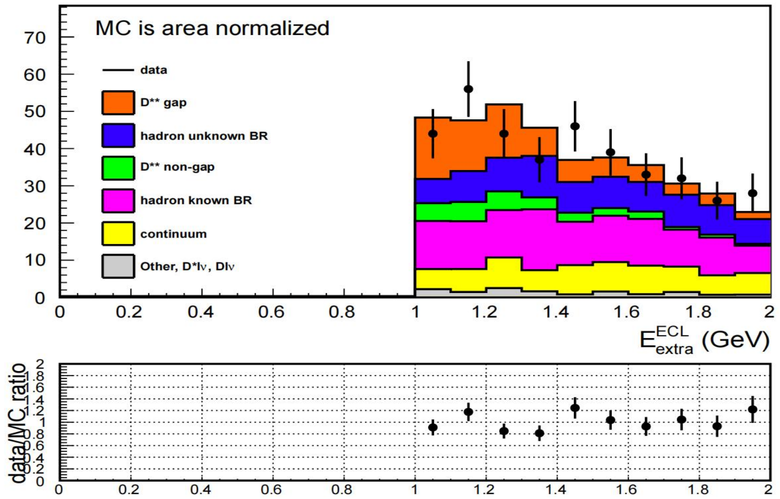

$(d) B^- \to D^{*0}\tau^-\bar{\nu}_{\tau^-} (D^{*0} \to D^0\gamma^0)$

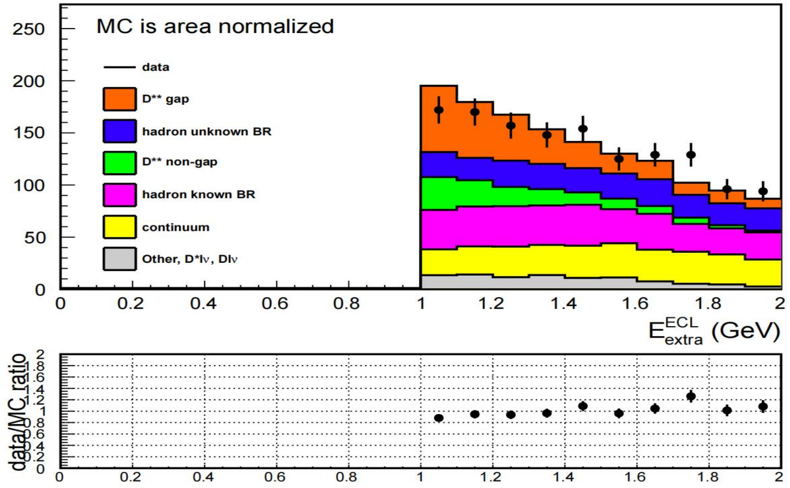

$(e) B^- \to D^0\tau^-\bar{\nu}_{\tau^-}$

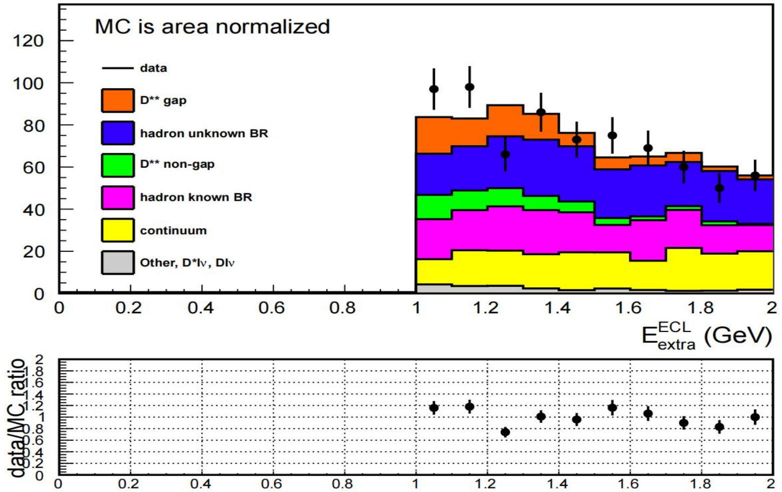

$(f) B^0 \to D^+\tau^-\bar{\nu}_{\tau^-}$

Signal extraction

generator level categorization

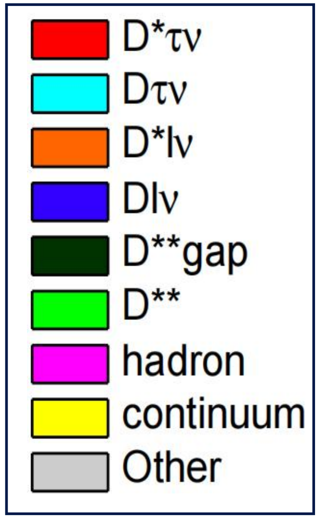

- PDF category is updated not to use “isSignal” but generator information

  9 PDF category

- Binning is updated to reduce MC statistics error

  $E_{\mathrm{extra}}^{\mathrm{ECL}}$ for all samples:

  [0.00, 0.05, 0.10, 0.2, 0.3, 0.4, 0.6, 0.8, 1.0, 2.0] GeV

  M_{miss}^{2} for all samples:

  [-2, -0.5, 0.0, 0.5, 1.0, 1.5, 2.0, 3.0, 4.0, 4.5, 5.0, 6.0, 7.0, 8.0, 10.0] GeV^2

- fit 5 samples:

  $B^0 \rightarrow \mathrm{D}^{*+}\tau\nu$(combined $\mathrm{D}^{*+} \rightarrow \mathrm{D}^0\pi^+$ and $\mathrm{D}^{*+} \rightarrow \mathrm{D}^+\pi^0$)

  $B^+ \rightarrow \mathrm{D}^{*0}\tau\nu$, $\mathrm{D}^{*0} \rightarrow \mathrm{D}^0\pi^0$

  $B^+ \rightarrow \mathrm{D}^{*0}\tau\nu$, $\mathrm{D}^{*0} \rightarrow \mathrm{D}^0\gamma$

  $B^0 \rightarrow \mathrm{D}^{+}\tau\nu$

  $B^- \rightarrow \mathrm{D}^{0}\tau\nu$

Data fitting

- pre/post fit parameters

$BR(B -> D^*\ell\nu)$ is larger than MC expectation with statistical error

number of gap mode ($N(\text{gap})$) is smaller than MC expectation

Table 9.4: Fitted parameters to the selected events

parameters	prefit	postfit with stat. error
$R(D^*)$	–	0.242 ± 0.019
$R(D)$	–	0.439 ± 0.055
$BR(B \to D^*\ell\nu)$	0.1013	0.1101 ± 0.0025
$BR(B \to D\ell\nu)$	0.0437	0.0431 ± 0.0013
$N(\text{gap mode}),\ B^0 \to D^{*+}\tau\nu$	118.27	21.4 ± 24.8
$N(\text{gap mode}),\ B^+ \to D^{*0}\tau\nu(D^{*0} \to \pi^0 D^0)$	70.996	41.6 ± 15.1
$N(\text{gap mode}),\ B^+ \to D^{*0}\tau\nu(D^{*0} \to \gamma D^0)$	229.43	53.4 ± 49.6
$N(\text{gap mode}),\ B^+ \to D^0\tau\nu$	776.79	240.3 ± 93.5
$N(\text{gap mode}),\ B^0 \to D^+\tau\nu$	271.10	89.5 ± 46.4
$N(D^{**}\ell\nu),\ B^0 \to D^{*+}\tau\nu$	110.70	60.1 ± 31.2
$N(D^{**}\ell\nu),\ B^+ \to D^{*0}\tau\nu(D^{*0} \to \pi^0 D^0)$	46.964	28.9 ± 23.9
$N(D^{**}\ell\nu),\ B^+ \to D^{*0}\tau\nu(D^{*0} \to \gamma D^0)$	206.19	190.5 ± 58.3
$N(D^{**}\ell\nu),\ B^+ \to D^0\tau\nu$	774.99	731.1 ± 134.0
$N(D^{**}\ell\nu),\ B^0 \to D^+\tau\nu$	283.32	294.2 ± 63.5
$N(\text{hadronic } B\ ),\ B^0 \to D^{*+}\tau\nu$	98.644	86.0 ± 25.3
$N(\text{hadronic } B\ ),\ B^+ \to D^{*0}\tau\nu(D^{*0} \to \pi^0 D^0)$	41.766	3.5 ± 12.2
$N(\text{hadronic } B\ ),\ B^+ \to D^{*0}\tau\nu(D^{*0} \to \gamma D^0)$	157.28	165.6 ± 38.2
$N(\text{hadronic } B\ ),\ B^+ \to D^0\tau\nu$	566.68	469.2 ± 94.6
$N(\text{hadronic } B\ ),\ B^0 \to D^+\tau\nu$	266.88	125.6 ± 25.3
f_{00}	0.4861 ± 0.0080	0.4861 ± 0.0080
f_{+-}	0.5113 ± 0.0108	0.5113 ± 0.0108
$N_{B\overline{B}}$	387.1 ± 5.6	387.1 ± 5.6

Data fitting

- Measured $BR(B -> D^*\ell\nu)$ is consistent with past measurements within systematic error：
- PDG(1.2σ)
- input to FEI calibration (HFLAV 2022) (0.4σ)
- q2 sideband (1.4σ)

Table 9.2: Comparison of the measured BR($B \to D^{(*)}\ell\nu$) with this analysis and previous measurements. HFLAV 2022 is used for input of FEI efficiency calibration analysis of $B \to X_\ell\nu$. Sum of $BR(B^0 \to D^{(*)}\ell\nu)$ and $BR(B^+ \to D^{(*)}\ell\nu)$ are shown.

	pdg live	HFLAV 2022	this analysis q^2 sideband	this analysis selected events
$BR(B \to D^*\ell\nu)$	0.1013 ±0.0013 (stat.+sys.)	0.1071 ±0.0026 (stat.+sys.)	0.1038 ±0.0027(stat.) ±0.0070(sys.)	0.1101 ±0.0025(stat.) ±0.0070(sys.)
$BR(B \to D\ell\nu)$	0.0436 ±0.0010 (stat.+sys.)	0.0466 ±0.0013 (stat.+sys.)	0.0436 ±0.0012(stat.)	0.0431 ±0.0013(stat.)

Data fitting

- To enhance the signal contribution in the E_{ECL} distribution, the additional requirement $M_{miss}^{2} > 1.5\ \mathrm{GeV}^2/c^2$ is imposed for D^* modes and $M_{\mathrm{miss}}^{2} > 2\ \mathrm{GeV}^2/c^2$ is imposed for D modes
- In the M_{miss}^{2} plots, the y-axis is zoomed.

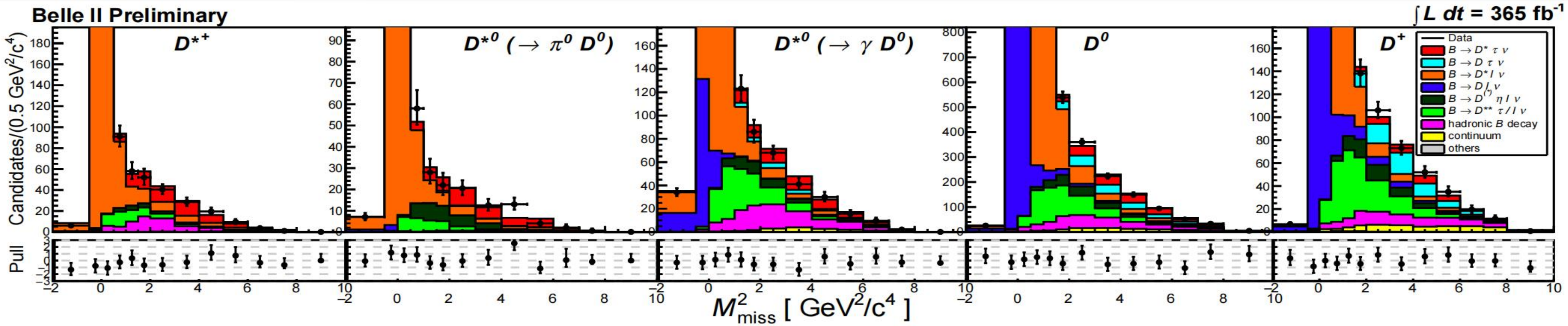

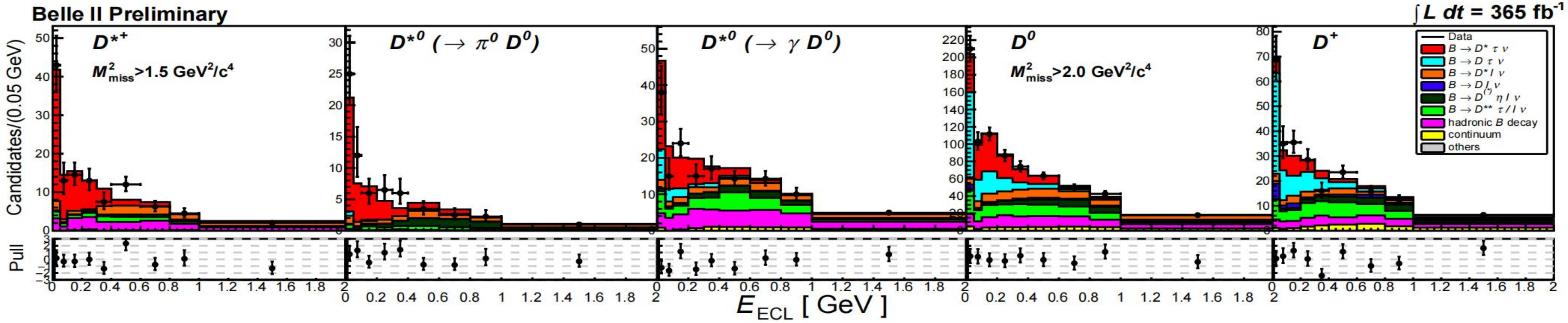

Data fitting

- Summary of the uncertainties

Table II. Summary of the systematic uncertainties on $R(D^{(*)})$ and their correlation. The description of each source is provided in the text.

Source	$R(D^*)$	$R(D)$	ρ
Simulation sample size	4.8%	8.4%	−0.44
gap-mode branching fraction	2.6%	2.6%	0.00
$\bar{B} \to D^{**}\tau^-/(\ell^-)\bar{\nu}_\ell$ branching fractions	0.3%	1.3%	0.25
Hadronic B decay branching fractions	1.6%	1.5%	−0.26
Form factors	0.5%	0.9%	−0.70
Continuum background	2.4%	2.1%	0.93
Fraction of fake $D^{(*)}$	0.5%	1.2%	0.00
Fit bias	0.3%	1.2%	0.00
Low-momentum π^0, γ efficiency	2.2%	2.4%	0.99
Other efficiency corrections	0.5%	0.8%	0.48
B-tagging efficiency of data	0.9%	1.8%	−1.00
B-tagging efficiency of $B \to D\tau\nu$	0.1%	1.8%	1.00
M^2_{miss} resolution	0.5%	0.8%	0.48
Total systematic uncertainty	6.7%	10.2%	−0.11
Statistical uncertainty	8.3%	16.3%	−0.40

- Result of fit

$$R(D^*) = 0.242 \pm 0.019(\text{stat.}) \pm 0.016(\text{syst}).\ R(D) = 0.439 \pm 0.055(\text{stat.}) \pm 0.045(\text{syst.})$$

$$\rho = -0.40(\text{stat.}) + 0.20(\text{syst.})$$

Data fitting

- The 68% confidence-level region in the $R(D) - R(D^*)$ plane from this analysis, compared with previous BelleII measurements , the world average, and the SM predictions

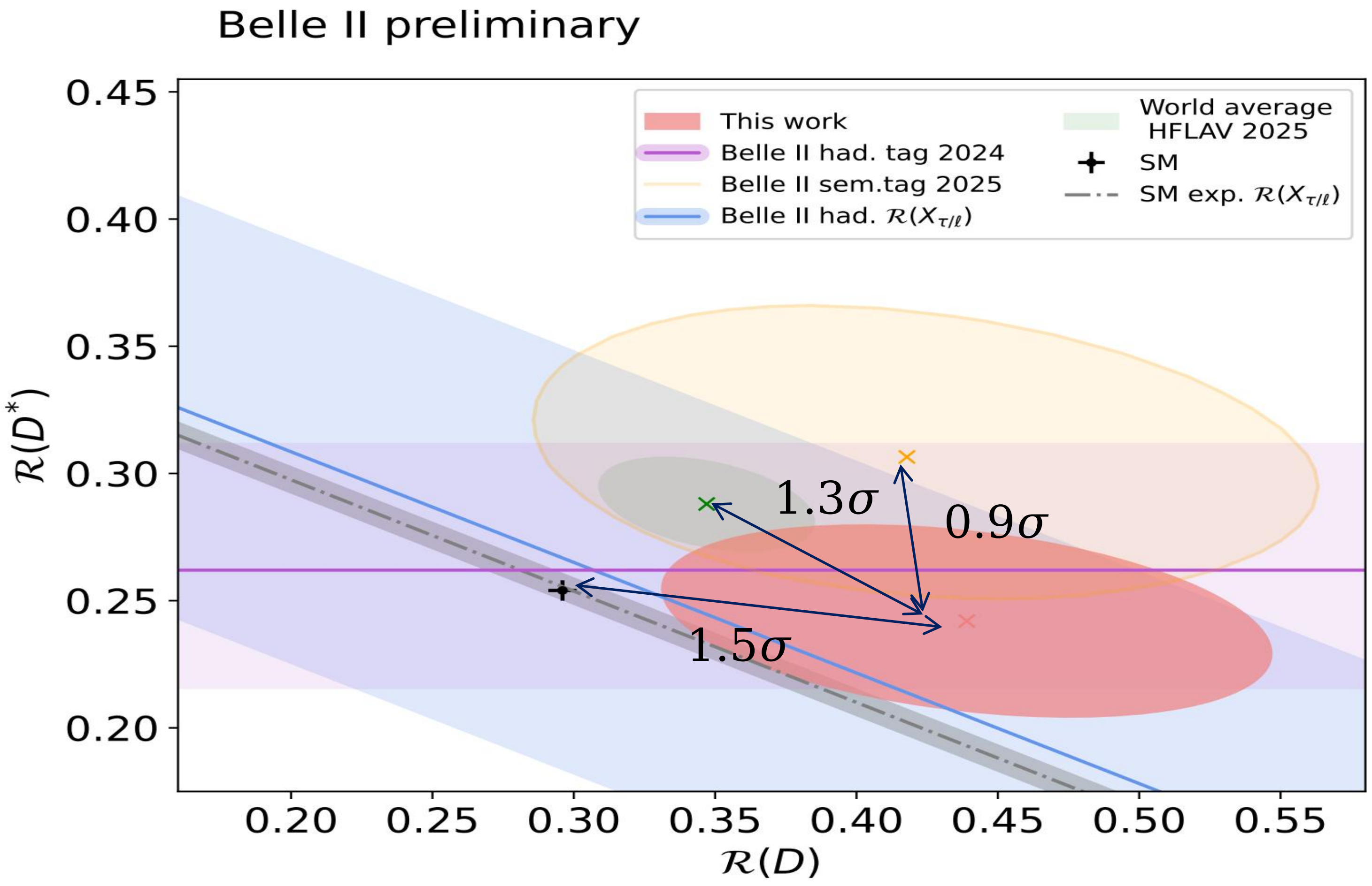

When included in the world average, our results reduce the deviation from the SM from 3.8σ to 3.6σ.

Summary

- R$(D^{(*)})$ measurement with hadronic tag:

$$R(D^{*}) = 0.242 \pm 0.019(\text{stat.}) \pm 0.016(\text{syst.})$$

$$R(D) = 0.439 \pm 0.055(\text{stat.}) \pm 0.045(\text{syst.})$$

$$\rho = -0.40(\text{stat.}) + 0.20(\text{syst.})$$

- When included in the world average, our results reduce the deviation from the SM from 3.8σ to 3.6σ.
- CWR1 is on-going

Back Up

Asimov Fit: $M^2_{\mathbf{miss}}$

- Asimov fit projection to the M^2_{miss} in each sample

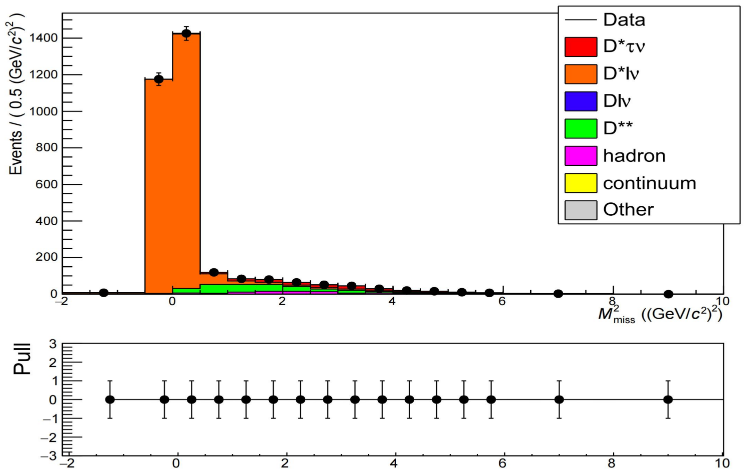

$(a) B^0 \text{->} \mathrm{D}^{*+}\tau^-\bar{\nu}_{\tau^-}(\mathrm{D}^{*+} \text{->} \mathrm{D}^0\pi^+/\mathrm{D}^+\pi^0)$

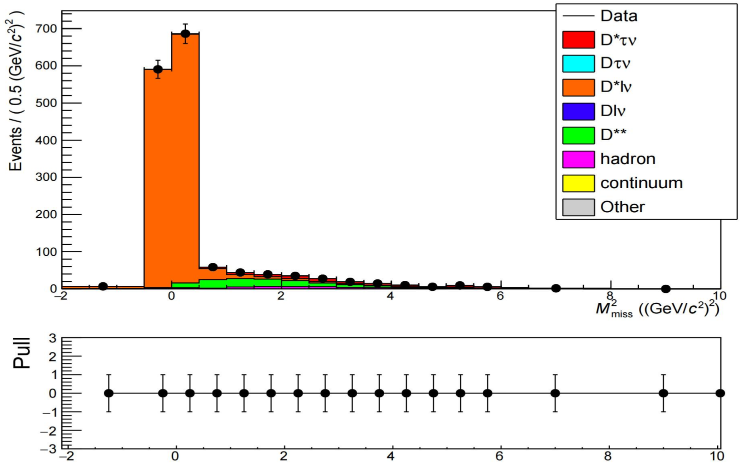

$(c) B^- \text{->} \mathrm{D}^{*0}\tau^-\bar{\nu}_{\tau^-}(\mathrm{D}^{*0} \text{->} \mathrm{D}^0\pi^0)$

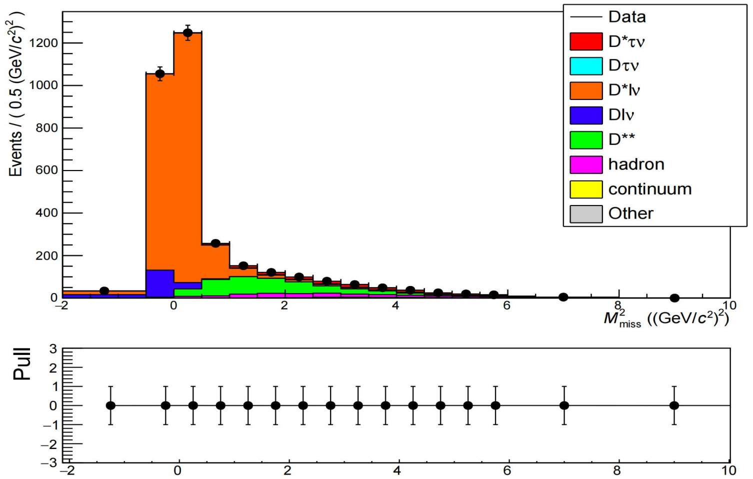

$(d) B^- \text{->} \mathrm{D}^{*0}\tau^-\bar{\nu}_{\tau^-}(\mathrm{D}^{*0} \text{->} \mathrm{D}^0\gamma^0)$

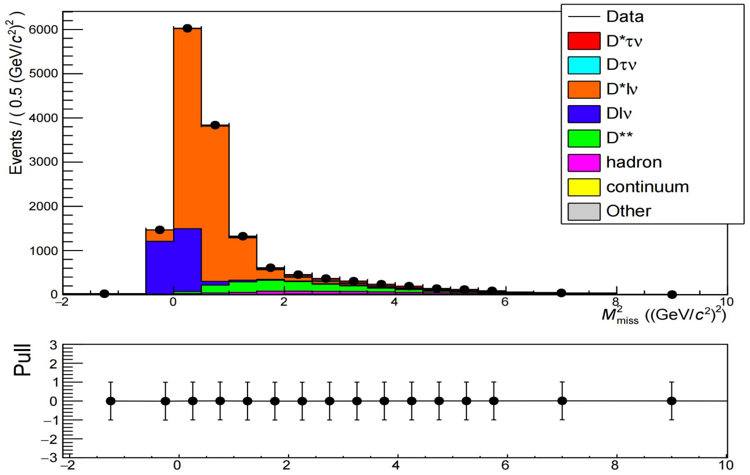

$(e) B^- \text{->} \mathrm{D}^0\tau^-\bar{\nu}_{\tau^-}$

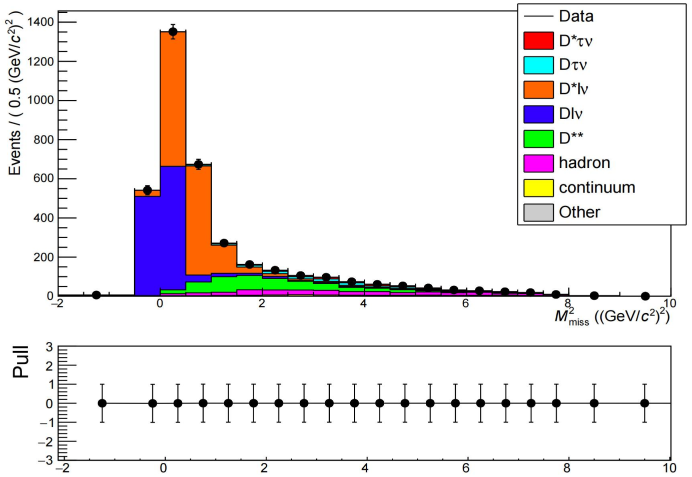

$(f) B^0 \text{->} \mathrm{D}^+\tau^-\bar{\nu}_{\tau^-}$

Asimov Fit: $E_{\mathbf{extra}}^{\mathbf{ECL}}$

- Asimov fit projection to the $E_{\mathrm{extra}}^{\mathrm{ECL}}$ in each sample

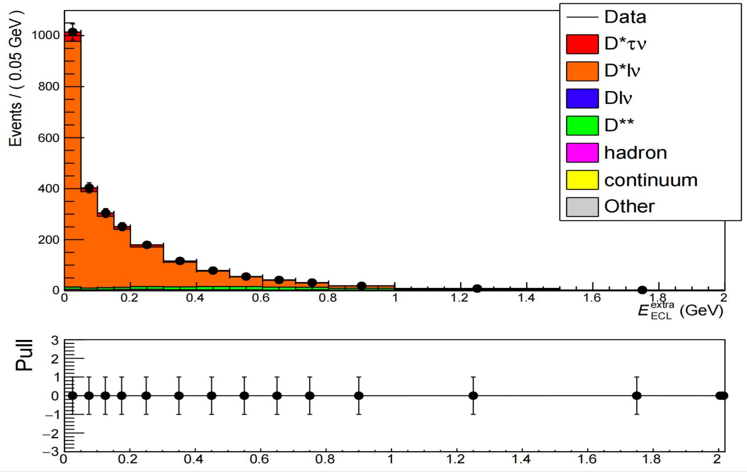

$(a) B^0 -> \mathrm{D}^{*+}\tau^-\bar{\nu}_{\tau^-}(\mathrm{D}^{*+} -> \mathrm{D}^0\pi^+/\mathrm{D}^+\pi^0)$

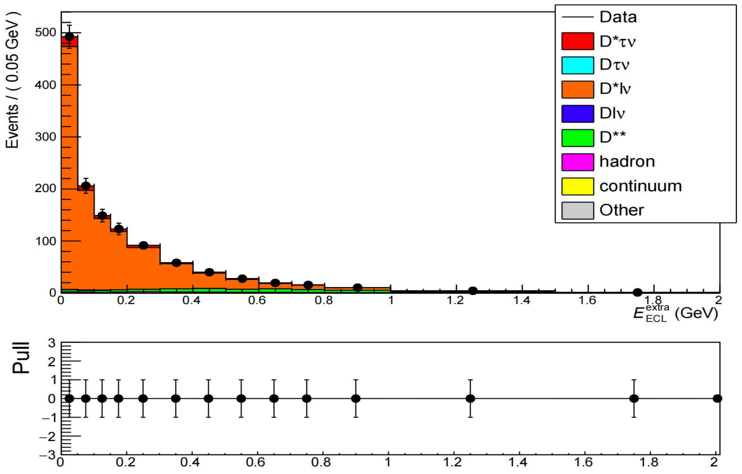

$(c) B^- -> \mathrm{D}^{*0}\tau^-\bar{\nu}_{\tau^-}(\mathrm{D}^{*0} -> \mathrm{D}^0\pi^0)$

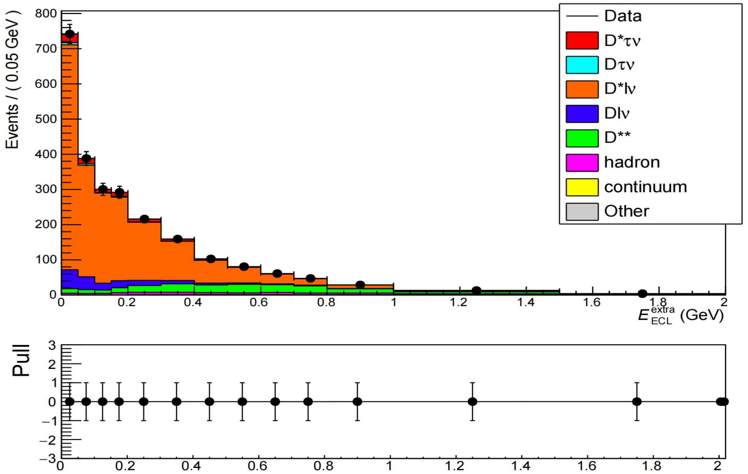

$(d) B^- -> \mathrm{D}^{*0}\tau^-\bar{\nu}_{\tau^-}(\mathrm{D}^{*0} -> \mathrm{D}^0\gamma^0)$

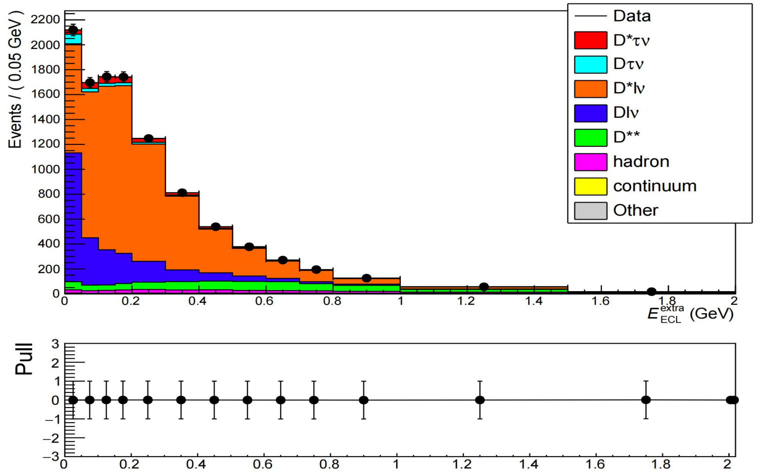

$(e) B^- -> \mathrm{D}^0\tau^-\bar{\nu}_{\tau^-}$

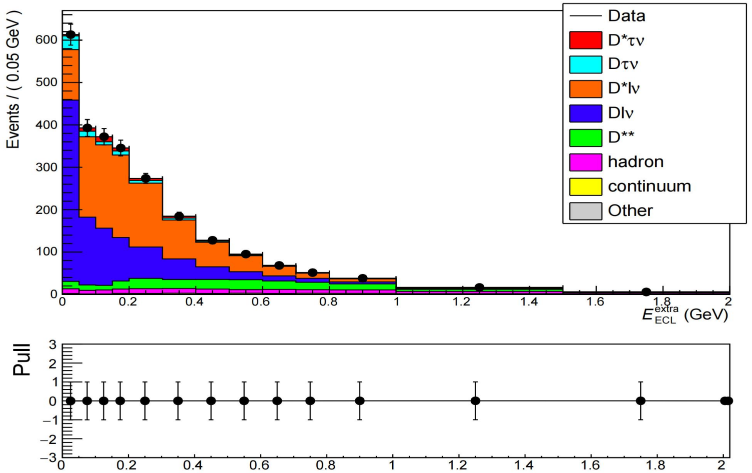

$(f) B^0 -> \mathrm{D}^+\tau^-\bar{\nu}_{\tau^-}$

Systematic error

- Summary of the systematic uncertainties

Table 7.1: Summary of the systematic uncertainties.

Error source	$R(D^*)$	$R(D)$	ρ
$\overline{B} \to D^{**}\ell^-\overline{\nu}_\ell$ branching fractions	0.6%	1.3%	0.02
MC statistics	4.2%	8.2%	-0.40
gap mode branching fractions $\pm 100\%$	0.1-6.5%	0.1-6.3%	0.0
gap mode branching fractions	1.6%	2.1%	-0.49
Hadronic B decay branching fractions	1.7%	2.9%	0.06
Continuum background	1.4%	1.9%	0.95
Slow π^0,γ efficiency	1.5%	3.0%	0.99
Other efficiency corrections	1.0%	1.0%	0.80
FEI efficiency of data	0.3%	1.1%	-1.0
FEI efficiency of $B \to D\tau\nu$	0.1%	2.4%	1.0
M^2_{miss} resolution	0.3%	0.9%	0.55
Fraction of fake $D^{(*)}$	0.7%	1.4%	0.08
Fitter bias	0.3%	1.4%	0.00
Form factors correction	0.4%	1.0%	-0.34
Total systematic uncertainty	5.1-8.3%	10.6-12.4%	-0.20

$\bar{B} \to D^{**}\ell^-\bar{\nu}$ branching fractions

- $D^{**}\ell\bar{\nu}$ branching ratio are taken from WG1's study with FLAV2023: GapUpdate.pdf
- gap mode of $B \to D^{(*)}\eta\ell\nu$ is largely changed from FLAV 2021:

  3.77±3.77 –> 8.8±8.8(B^0)

  4.09±4.09 –> 9.2±9.2(B^+)

Decay	BR in MC ($\times 10^{-3}$)	BR from HFLAV2023 ($\times 10^{-3}$)
$\overline{B}^0 \to D_0^{*+}(\to D\pi\pi)\ell^-\overline{\nu}_\ell$	– (8M events)	$(0.7 \pm 0.8)/2$
$\overline{B}^0 \to D_1'^{+}(\to D\pi\pi)\ell^-\overline{\nu}_\ell$	– (8M events)	$(0.7 \pm 0.8)/2$
$\overline{B}^0 \to D_0^{*+}(\to D^*\pi\pi)\ell^-\overline{\nu}_\ell$	– (8M events)	$(2.0 \pm 1.0)/2$
$\overline{B}^0 \to D_1'^{+}(\to D^*\pi\pi)\ell^-\overline{\nu}_\ell$	– (8M events)	$(2.0 \pm 1.0)/2$
$\overline{B}^0 \to D_0^{*+}(\to D\eta)\ell^-\overline{\nu}_\ell$	– (8M events)	8.8 ± 8.8
$\overline{B}^0 \to D_1'^{+}(\to D^*\eta)\ell^-\overline{\nu}_\ell$	– (8M events)	8.8 ± 8.8
$\overline{B}^0 \to D^{*0}\pi^+\ell^-\overline{\nu}_\ell$	0.92	0.30 ± 0.20
$\overline{B}^0 \to D^0\pi^+\ell^-\overline{\nu}_\ell$	0.92	0.30 ± 0.20
$\overline{B}^0 \to D^{*+}\pi^0\ell^-\overline{\nu}_\ell$	0.46	0.30 ± 0.20
$\overline{B}^0 \to D^+\pi^0\ell^-\overline{\nu}_\ell$	0.46	0.30 ± 0.20
$\overline{B}^0 \to D_1^+\ell^-\overline{\nu}_\ell$	7.04	5.9 ± 1.0
$\overline{B}^0 \to D_0^{*+}\ell^-\overline{\nu}_\ell$	3.62	1.2 ± 1.8
$\overline{B}^0 \to D_1'^{+}\ell^-\overline{\nu}_\ell$	4.01	2.6 ± 0.4
$\overline{B}^0 \to D_2^{*+}\ell^-\overline{\nu}_\ell$	3.47	2.99 ± 0.27
$\overline{B}^0 \to D_1^+\tau^-\overline{\nu}_\tau$	1.3	5.2 ± 5.2
$\overline{B}^0 \to D_0^{*+}\tau^-\overline{\nu}_\tau$	1.3	3.3 ± 3.3
$\overline{B}^0 \to D_1'^{+}\tau^-\overline{\nu}_\tau$	2.0	3.3 ± 3.3
$\overline{B}^0 \to D_2^{*+}\tau^-\overline{\nu}_\tau$	2.0	2.3 ± 2.3

$B^- \to D_0^{*0}(\to D\pi\pi)\ell^-\overline{\nu}_\ell$	– (8M events)	$(0.7 \pm 0.9)/2$
$B^- \to D_1'^{0}(\to D\pi\pi)\ell^-\overline{\nu}_\ell$	– (8M events)	$(0.7 \pm 0.9)/2$
$B^- \to D_0^{*0}(\to D^*\pi\pi)\ell^-\overline{\nu}_\ell$	– (8M events)	$(2.2 \pm 1.0)/2$
$B^- \to D_1'^{0}(\to D^*\pi\pi)\ell^-\overline{\nu}_\ell$	– (8M events)	$(2.2 \pm 1.0)/2$
$B^- \to D_0^{*0}(\to D\eta)\ell^-\overline{\nu}_\ell$	– (8M events)	9.2 ± 9.2
$B^- \to D_1'^{0}(\to D^*\eta)\ell^-\overline{\nu}_\ell$	– (8M events)	9.2 ± 9.2
$B^- \to D^{*0}\pi^0\ell^-\overline{\nu}_\ell$	0.50	0.30 ± 0.20
$B^- \to D^0\pi^0\ell^-\overline{\nu}_\ell$	0.50	0.30 ± 0.20
$B^- \to D^{*+}\pi^-\ell^-\overline{\nu}_\ell$	1.00	0.30 ± 0.20
$B^- \to D^+\pi^-\ell^-\overline{\nu}_\ell$	1.00	0.30 ± 0.20
$B^- \to D_s^{*+}K^-\ell^-\overline{\nu}_\ell$	0.30	0.29 ± 0.19
$B^- \to D_s^+K^-\ell^-\overline{\nu}_\ell$	0.30	0.30 ± 0.13
$B^- \to D_1^0\ell^-\overline{\nu}_\ell$	7.57	6.4 ± 1.0
$B^- \to D_0^{*0}\ell^-\overline{\nu}_\ell$	3.89	1.3 ± 1.9
$B^- \to D_1'^{0}\ell^-\overline{\nu}_\ell$	4.31	2.8 ± 0.4
$B^- \to D_2^{*0}\ell^-\overline{\nu}_\ell$	3.73	3.21 ± 0.29
$B^- \to D_1^0\tau^-\overline{\nu}_\tau$	1.3	5.6 ± 5.6
$B^- \to D_0^{*0}\tau^-\overline{\nu}_\tau$	1.3	3.6 ± 3.6
$B^- \to D_1'^{0}\tau^-\overline{\nu}_\tau$	2.0	3.6 ± 3.6
$B^- \to D_2^{*0}\tau^-\overline{\nu}_\tau$	2.0	2.5 ± 2.5

Hadronic B decay branching fractions

- The branching fractions of hadronic B decays are fluctuated following their errors in the following table

	Decay	decayModeID	$\mathcal{B}$ in MC $[10^{-3}]$	$\mathcal{B}$ in PDG $[10^{-3}]$
	$B^+ \to D_s^+ \overline{D}$	1681	9.0	9.0 ± 0.9
	$B^+ \to D_s^+ \overline{D}^*$	1682	8.2	8.2 ± 1.7
	$B^+ \to D_s^{*+} \overline{D}$	1683	7.6	7.6 ± 1.6
	$B^+ \to D_s^{*+} \overline{D}^*$	1684	17.1	17.1 ± 2.4
	$B^+ \to \overline{D_2^*}^0 D_s^+$	1689	4.2	–
	$B^+ \to \overline{D_2^*}^0 D_s^{*+}$	1690	4.0	–
	$B^+ \to \overline{D^{*0}} D^+$	1727	0.63	0.63 ± 0.17
	$B^+ \to \overline{D^0} D_{s0}^{*+}$	1764	7.6	–
	$B^+ \to \overline{D^0} D_{s1}^{\prime +}$	1773	0.45	0.4 ± 0.1
$D^{(*)}D^{(*)}$	$B^+ \to \overline{D^{*0}} D_{s1}^{\prime +}$	1774	0.94	0.94 ± 0.42
	$B^0 \to D_s^+ D^-$	1833	7.2	7.2 ± 0.8
	$B^0 \to D_s^+ D^{*-}$	1834	8.0	8.0 ± 1.1
	$B^0 \to D_s^{*+} D^-$	1835	7.4	7.4 ± 1.6
	$B^0 \to D_s^{*+} D^{*-}$	1836	17.7	17.7 ± 1.4
	$B^0 \to D_2^{*-} D_s^+$	1841	4.2	–
	$B^0 \to D_2^{*-} D_s^{*+}$	1842	4.0	–
	$B^0 \to D_{s0}^{*+} D^-$	1928	7.4	–
	$B^0 \to D_{s0}^{*+} D^{*-}$	1929	17.7	–
	$B^0 \to D_{s1}^{\prime +} D^-$	1939	3.5	3.5 ± 1.1
	$B^0 \to D_{s1}^{\prime +} D^{*-}$	1940	9.3	9.3 ± 2.2
	$B^+ \to \overline{D^0} D^+ K^0$	1701	1.55	1.55 ± 0.21
	$B^+ \to \overline{D^0} D^{*+} K^0$	1702	3.8	3.8 ± 0.4
	$B^+ \to \overline{D^{*0}} D^+ K^0$	1703	2.1	2.1 ± 0.5
	$B^+ \to \overline{D^{*0}} D^{*+} K^0$	1704	9.2	9.2 ± 1.2
	$B^+ \to \overline{D^0} D^{*0} K^+$	1707	6.3	6.3 ± 0.5
$D^{(*)}D^{(*)}K$	$B^+ \to \overline{D^{*0}} D^{*0} K^+$	1708	11.2	11.2 ± 1.3
	$B^0 \to D^{*-} D^{*0} K^+$	1856	10.6	10.6 ± 0.9
	$B^0 \to D^- D^+ K^0$	1857	0.75	0.75 ± 0.17
	$B^0 \to D^{*-} D^+ K^0$	1858	1.7	1.7 ± 0.1
	$B^0 \to D^- D^{*+} K^0$	1859	4.8	4.8 ± 0.4
	$B^0 \to D^{*-} D^{*+} K^0$	1860	8.1	8.1 ± 0.7
	$B^0 \to D^- D^+ K^{*0}$	1869	2.5	–
	$B^0 \to D^{*-} D^{*+} K^{*0}$	1872	5.0	–
	$B^+ \to D_s^+ \overline{D^0} \pi^0$	1692	1.8	–
	$B^+ \to D_s^{*+} \overline{D^0} \pi^0$	1694	1.8	–
	$B^+ \to \overline{D^{*-}} \pi^0 \pi^+ \pi^+$	1746	15	15 ± 7
	$B^+ \to \rho^+ \overline{D^0}$	1731	13.4	13.4 ± 1.8
	$B^+ \to \rho^+ \overline{D^{*0}}$	1732	9.8	9.8 ± 1.7
	$B^+ \to \overline{D^{*0}} a_1^+$	1740	19	19 ± 5
$D^* n\pi(\pi^0)$ etc.	$B^0 \to D_s^+ D^- \pi^0$	1845	1.8	–
	$B^0 \to D_s^{*+} \overline{D^0} \pi^-$	1846	3.7	–
	$B^0 \to D_s^+ D^- \pi^0 \pi^0$	1848	2.2	–
	$B^0 \to \rho^+ D^-$	1879	7.6	7.6 ± 1.2
	$B^0 \to \rho^+ D^{*-}$	1880	6.8	6.8 ± 0.9
	$B^0 \to D^{*-} \pi^+ \pi^0$	1882	8.35	8.2 ± 0.5
	$B^0 \to a_1^+ D^-$	1886	6.0	6.0 ± 3.3
	$B^0 \to a_1^+ D^{*-}$	1893	13.0	13.0 ± 0.27
	$B^0 \to D^* \pi^+ \pi^+ \pi^- \pi^0$	1998	17.6	17.6 ± 2.7
	$B^0 \to D^{*-} p^+ \overline{n^0}$	1990	1.5	–

If the measured branching ratio is not available on PDG, they are fluctuated ± 100% by uniform function.

FEI efficiency

- Weight is applied in each B_{tag} mode to scale MC to match data in q^2 sideband
- Difference of fit result is assigned as systematics

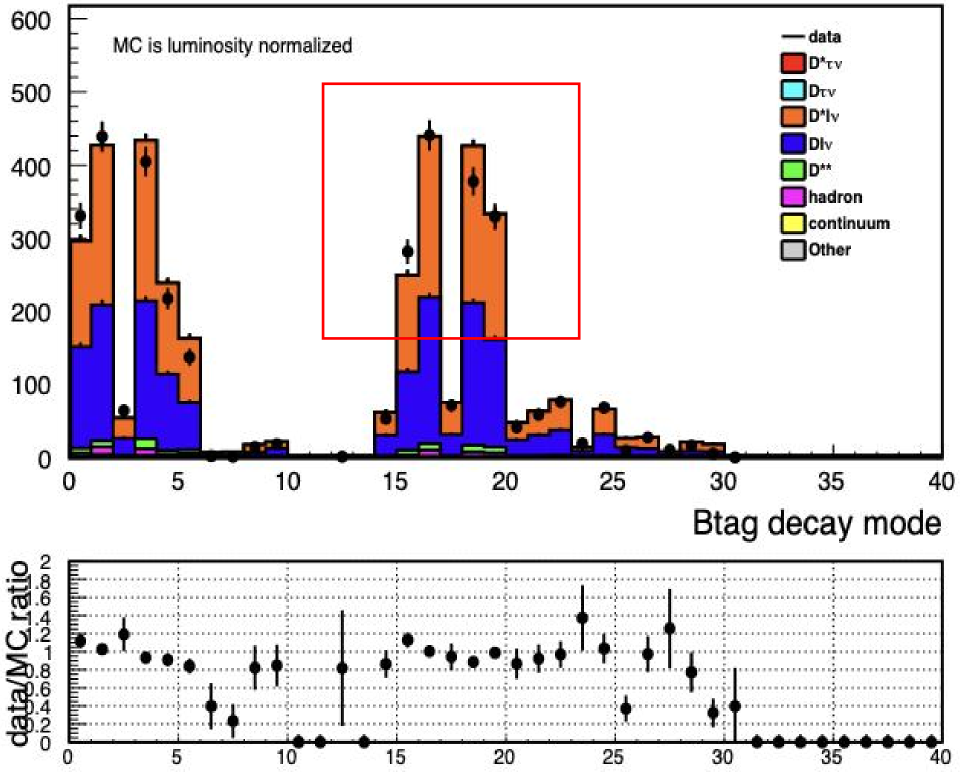

(a) B^0_{tag}

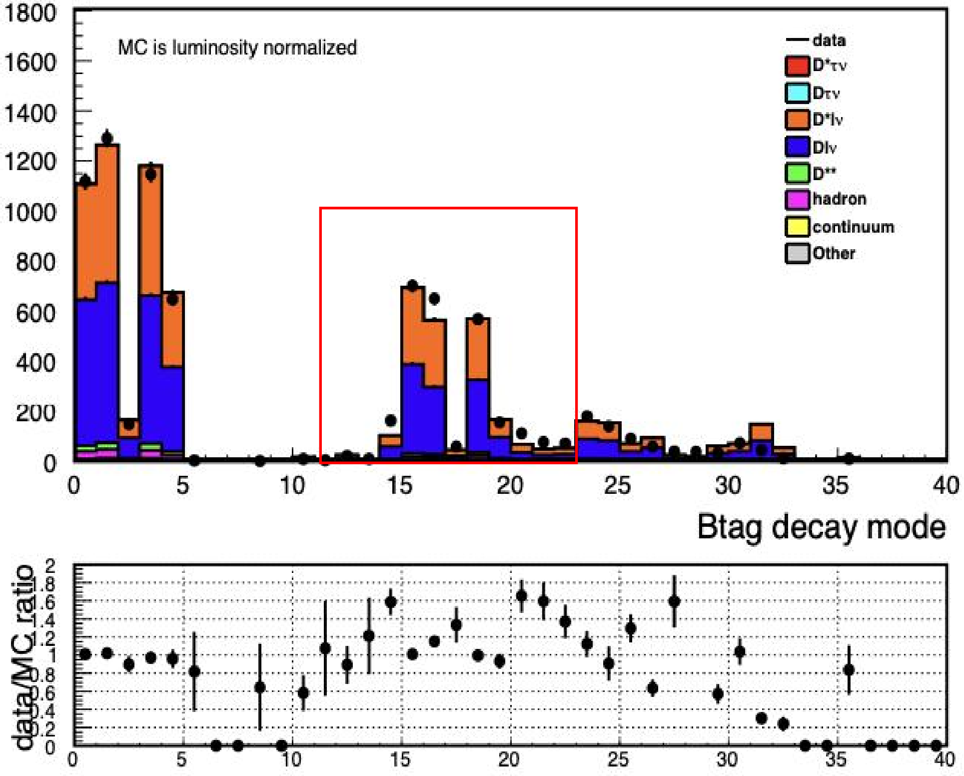

(b) B^+_{tag}

Other efficiency corrections

- Uncertainty of below correction are estimated:

  hadron PID correction

  lepton PID correction

  slow $\pi^{\pm}$ efficiency

  γ efficiency

  π^{0} efficienc

  mode-dependent FEI efficiency

From factors correction

The weights for translating the form factor uncertainties to the shape uncertainties of semileptonic B decays are defined as:

$$w_i = \frac{\Gamma_{\rm MC}}{\Gamma_{\rm new}} \times \frac{d\Gamma_{\rm new}}{d\Gamma_{\rm MC}}$$

- Update the form factor model from R(D*)@189 fb-1, e.g. BLPRXP is used to replace BGL and CLN
- Weights: normal weight +/- 1σ weights x No. parameters
- The event weights are calculated by Hammer

Semileptonic B decay	Form factor model		Parameters	
	MC14ri	MC15rd	MC14ri	MC15rd
$\bar{B} -> D\ell^-\bar{\nu}_\ell$	BGL	BLPRXP	8	9
$\bar{B} -> D^*\ell^-\bar{\nu}_\ell$	BGL	BLPRXP	6	9
$\bar{B} -> (D_0^*, D_1^{'})\ell^-\bar{\nu}_\ell$	LLSW	BLR	3	3
$\bar{B} -> (D_1, D_2^*)\ell^-\bar{\nu}_\ell$	LLSW	BLR	4	4
$\bar{B} -> D\tau^-\bar{\nu}_\ell$	CLN	BLPRXP	3	9
$\bar{B} -> D^*\tau^-\bar{\nu}_\ell$	CLN	BLPRXP	5	9
$\bar{B} -> (D_0^*, D_1^{'})\tau^-\bar{\nu}_\tau$	LLSW	BLR	3	3
$\bar{B} -> (D_1, D_2^*)\tau^-\bar{\nu}_\tau$	LLSW	BLR	4	4

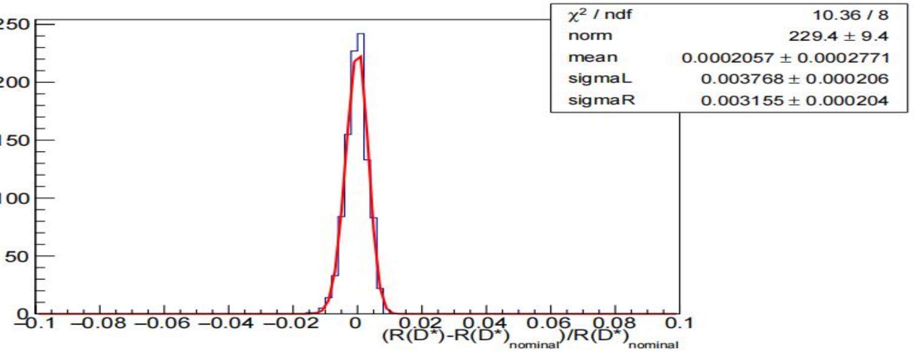

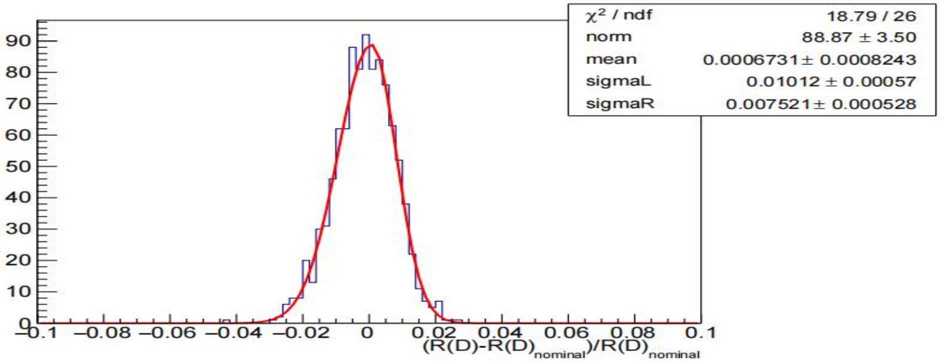

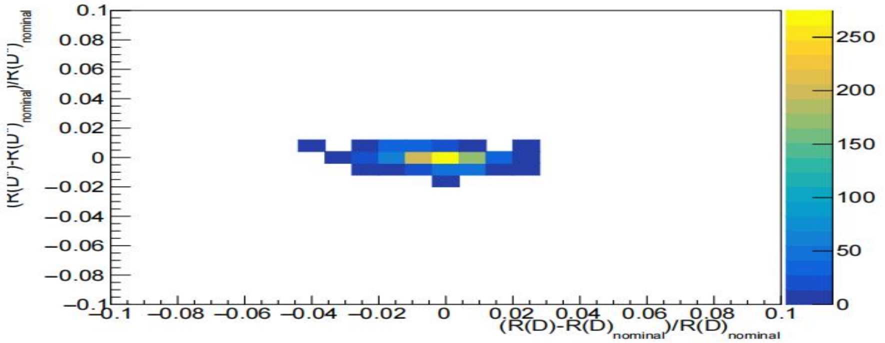

Fraction of fake $D^{(*)}$

- There is peaking structure in $D^{*+} \rightarrow D^0\pi^+$, $D^{*+} \rightarrow D^+\pi^0$, $D^{*0} \rightarrow D^0\pi^0$
- The fraction of correctly reconstructed $D^{(*)}$ is reweighted following the fit results at q^2 sideband and PDF is regenerated, then Asimov fit is performed.

Table 7.5: Data/MC comparison of the number of selected events at q^2 side-band. The error shows statistical error of data. systematic error is not included in the error.

Category	Fraction of correctly reconstructed $D^*)$					
	$D^{*+} \to D^0\pi^+$	$D^{*+} \to D^+\pi^0$	$D^{*0} \to D^0\pi^0$	$D^{*0} \to D^0\gamma$	D^0	D^+
before fit	0.929	0.853	0.850	0.500	0.907	0.919
after fit	1.000 $\pm$ 0.043	0.831 $\pm$ 0.137	1.000 $\pm$ 0.151	0.501 $\pm$ 0.070	0.865 $\pm$ 0.034	0.892 $\pm$ 0.065

Selection: ROE

- $E_{\mathrm{extra}}^{\mathrm{ECL}}$ shape is much cleaned than the last analysis

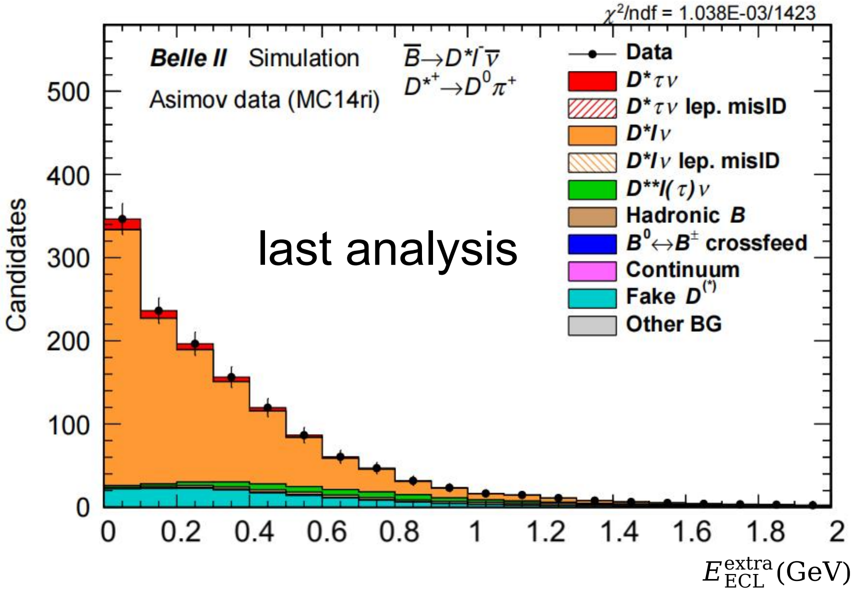

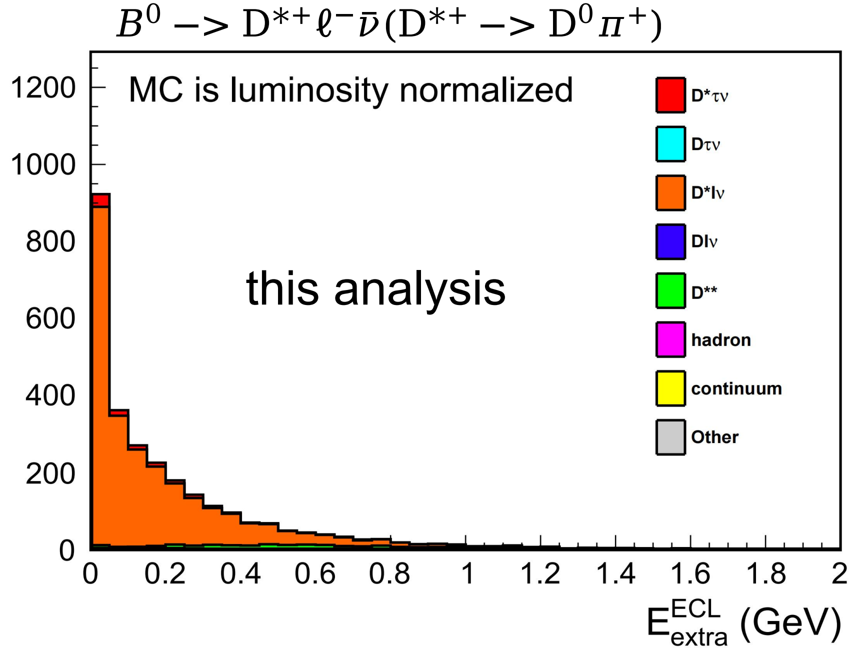

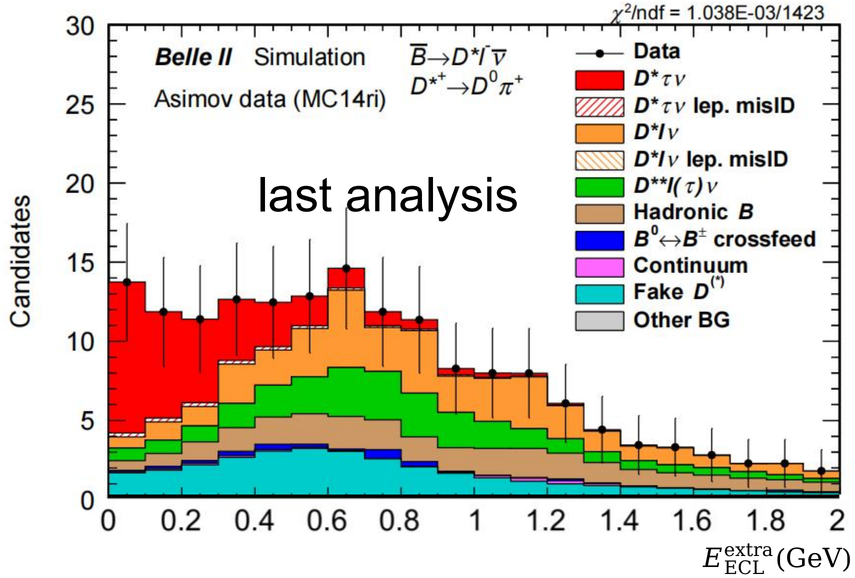

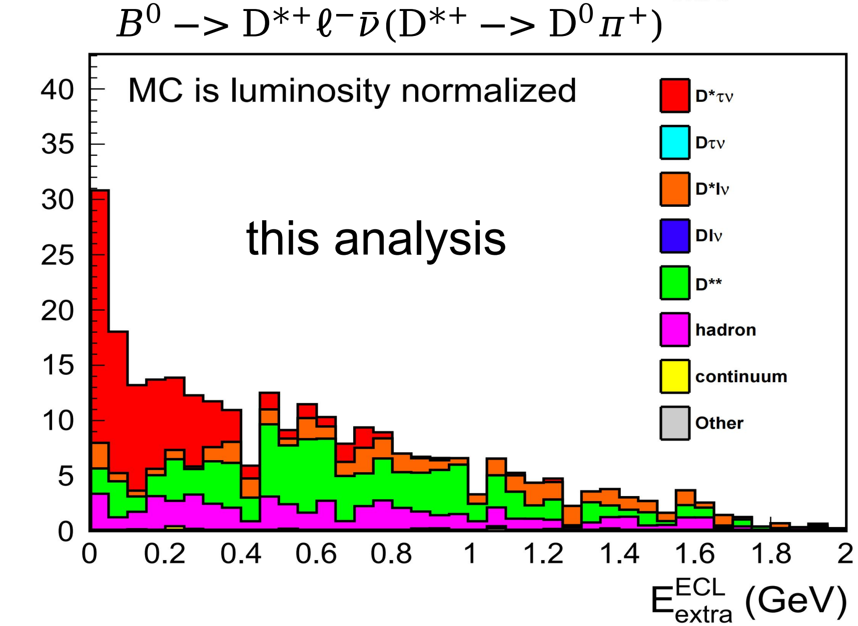

Selection: BCS

- There are multiple candidates in an event after the selections
- A best candidate selection is thus applied following five steps in following orders:

1、B_{tag} probability with the highest p_{FEI}

2、$D^{(*)}$ mode selection: $D^{*+} -> D^0\pi^+$, $D^{*+} -> D^+\pi^0$, $D^{*0} -> D^0\pi^0$, $D^{*0} -> D^0\gamma$, D^0, D^+

3、$D^{(*)}$ mode dependent selection: smallest χ^2

4、D branch ration

5、Random: for events still have multuiple candidates. The best candidate is selected randomly(~1.7%)

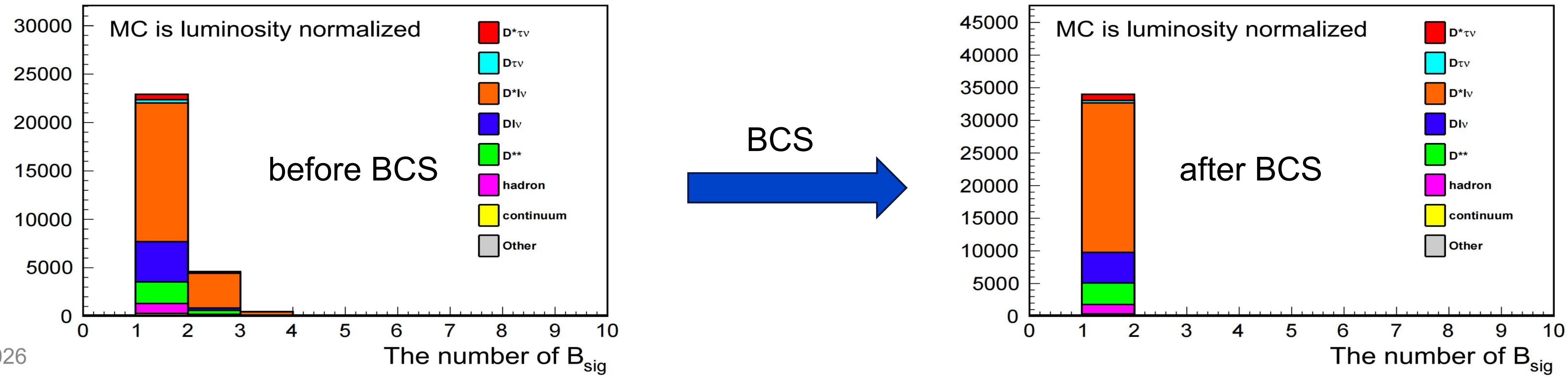

q^2 sideband

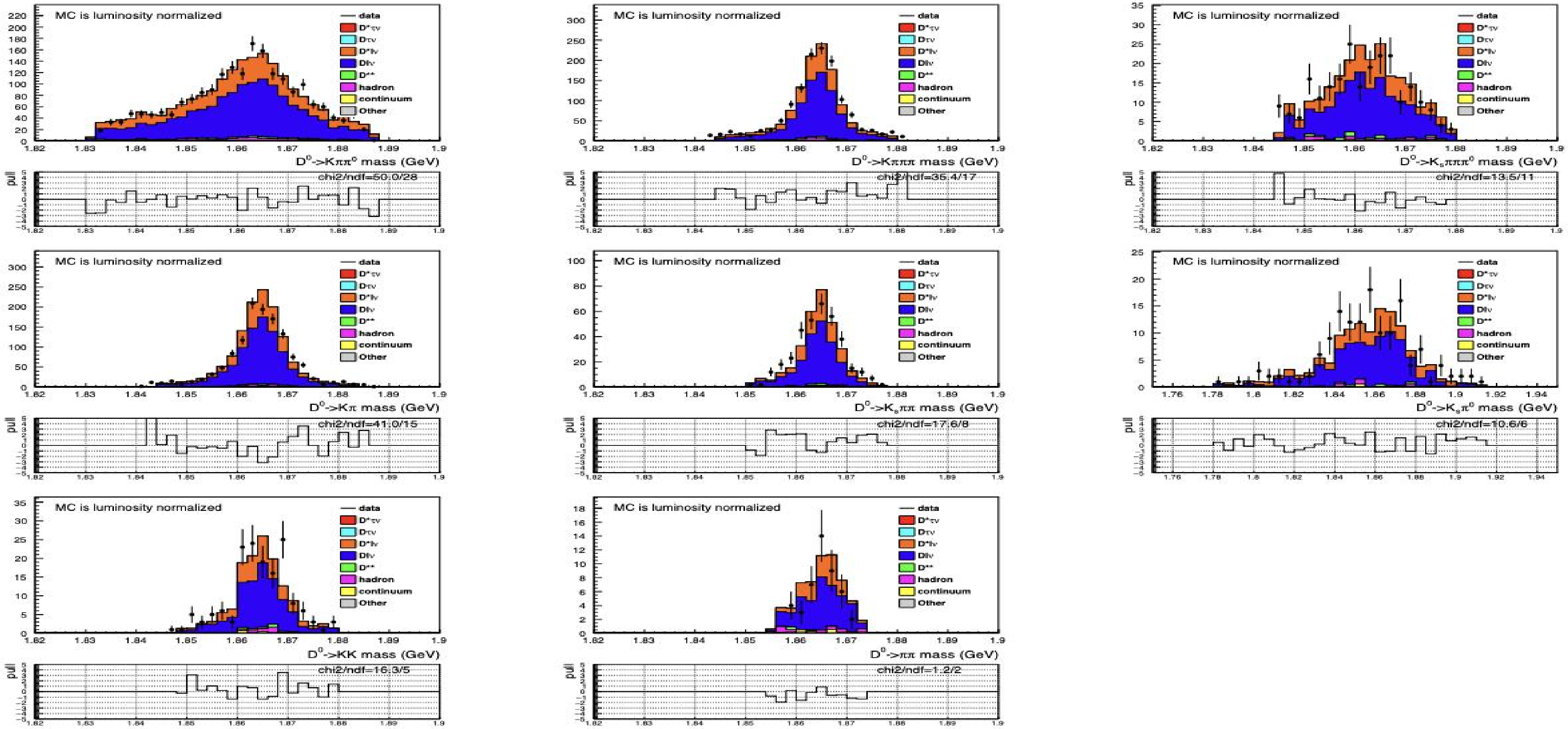

Figure 5.1: Invariant mass of D^0 in each decay mode at q^2 sideband with all selections including the mass selection.

q^2 sideband

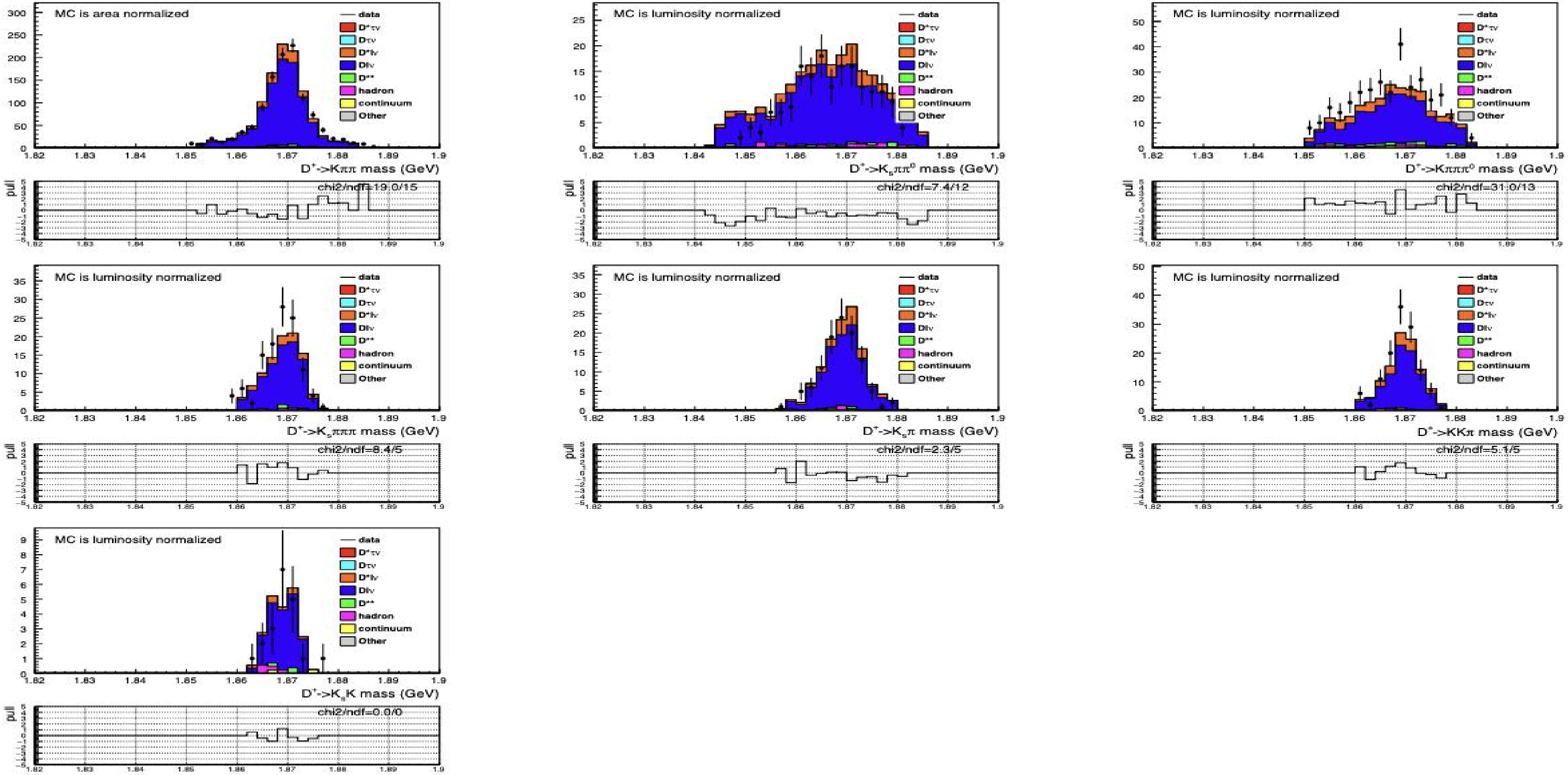

Figure 5.2: Invariant mass of D^+ in each decay mode at q^2 sideband with all selections including the mass selection.

q^2 sideband

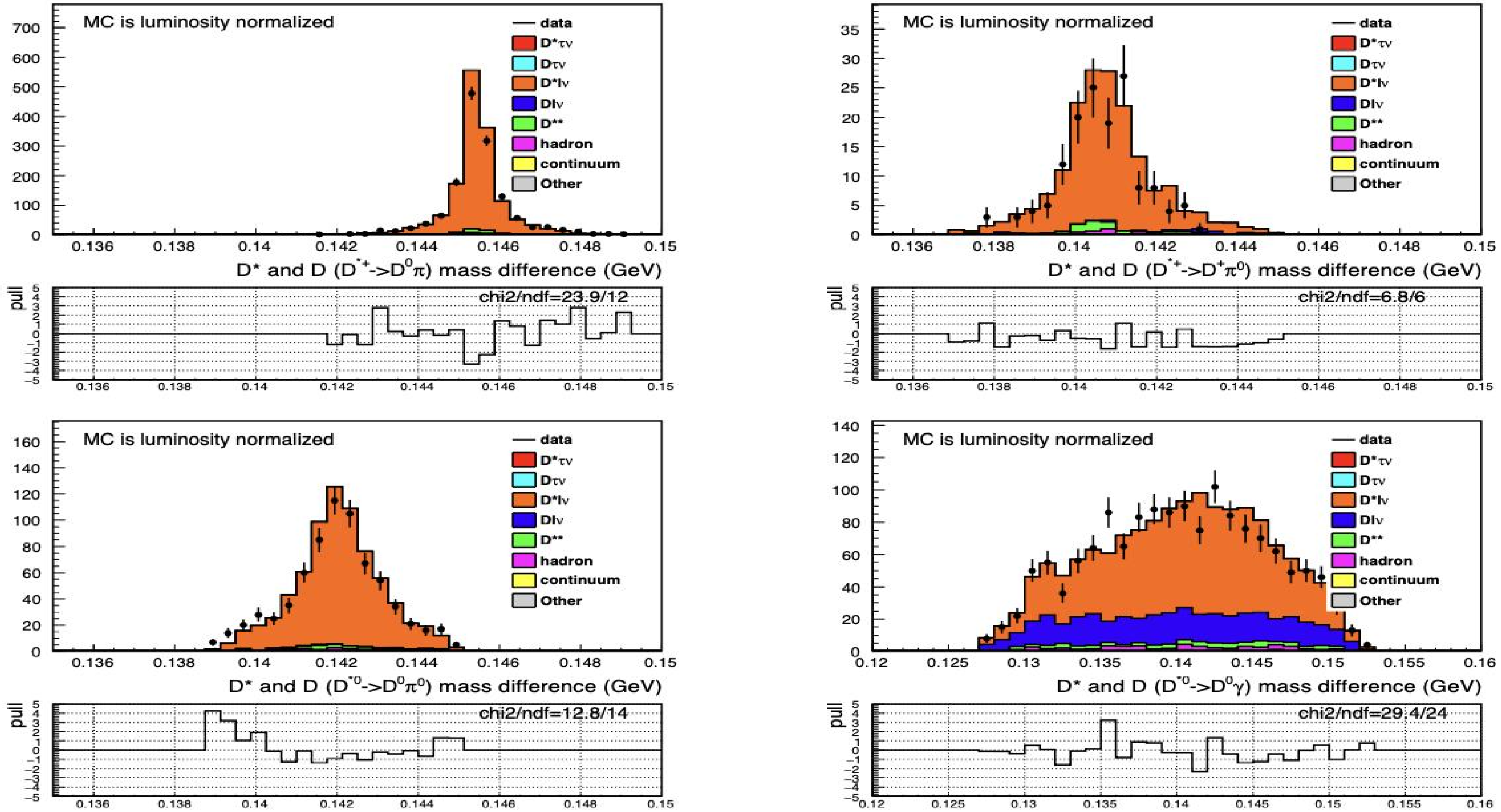

Figure 5.3: Mass differences of D^* and D in each decay mode at q^2 sideband with all selections including the mass selection.

Fited bias

- The fitter bias is seen depends on $R(D^*)$ and $R(D)$ input values
- The maximum bias in the figure is taken as systematic error

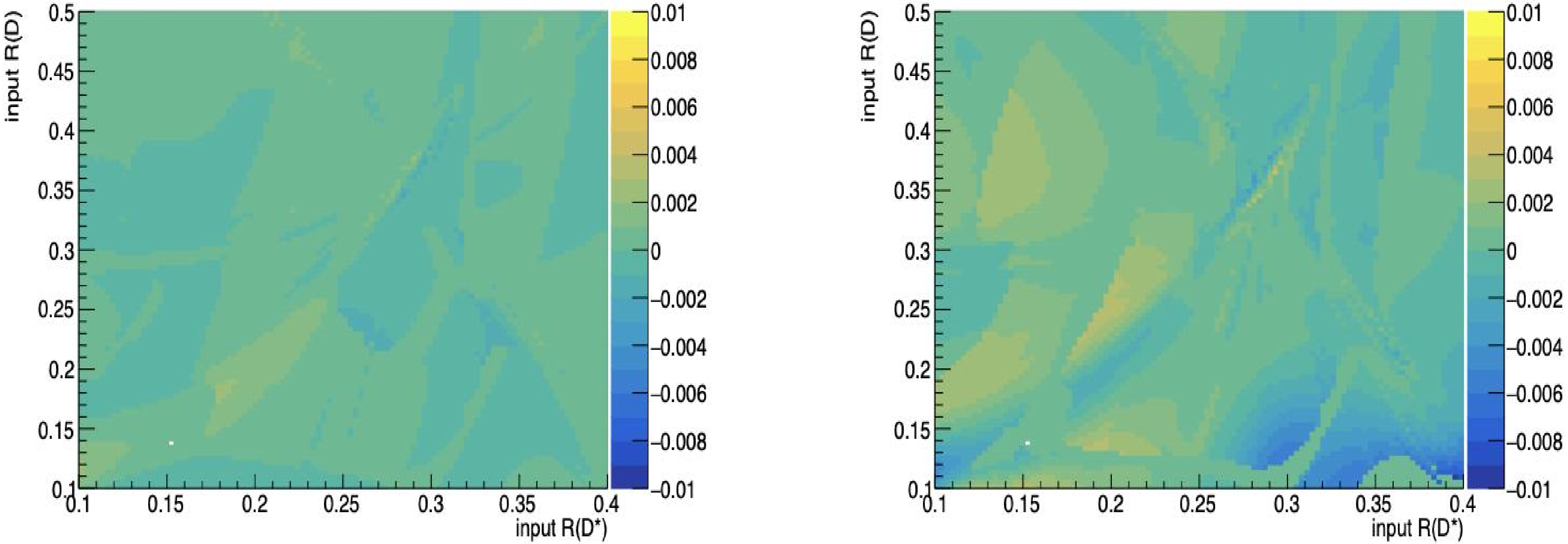

Fitter bias of $R(D^*)$(left) and $R(D)$(right) with Asimov fit. x and y axisare input value of $R(D^*)$ and $R(D)$, and z axis is the bias defined as $(R(D^{(*)}) - R(D^{(*)})_{\text{input}})/R(D^{(*)})_{\text{input}}$

Correction of branching ratios

- Values of the branching ratios of signal and background are different between the Belle II simulation and PDG
- The differences are evaluated and corrections are applied to MC

  branching ratio of $B -> D^{(*)}\ell\nu$

  branching ratio of $\tau -> \ell\nu\bar{\nu}$

  branching ratio of $D*$

  branching ratio of D

  branching ratio of hadronic B decay

  branching ratio of $B -> D^{**}\ell\nu$ decay

Expected Yields

Expected Yields

Expected Yields